Investigations of structure and dynamics of [1.1]ferrocenophanes and their alkali metal salts

Unravelling of the detailed mechanism of an alkali metallation reaction and the conformational properties of [1.1]ferrocenophanes by NMR-, UV-vis-spectroscopy and X-ray diffraction

by

Jan-Martin Löwendahl

Department of Organic Chemistry
Göteborg University
Göteborg, Sweden
1995

Investigations of structure and dynamics of [1.1]ferrocenophanes and their alkali metal salts

Unravelling of the detailed mechanism of an alkali metallation reaction and the conformational properties of [1.1]ferrocenophanes by NMR-, UV-vis-spectroscopy and X-ray diffraction

by

Jan-Martin Löwendahl

Department of Organic Chemistry
Göteborg University
S-412 96 Göteborg
1995

Akademisk avhandling
för avläggande av filosofie doktors examen i kemi, som enligt dekanus beslut kommer att försvaras offentligt fredagen den 17 mars 1995 kl 10.15 i föreläsningssal KA, Kemigården 3, Göteborgs Universitet och Chalmers Tekniska Högskola.

Fakultetsopponent är Docent Dan Johnels,
Institutionen för Organisk kemi, Umeå Universitet.
Avhandlingen försvaras på svenska.

ABSTRACT

Insight into the detailed mechanism of alkali metallation reactions has been obtained using 1-[1.1]ferrocenophanyllithium (**2**) and the corresponding sodium, potassium and cesium salts. These compounds undergo fast degenerate intramolecular 1,12-carbon metallation. The importance of aggregation, ion pairing, gegenion, solvation and to some extent the carbanion have been studied.

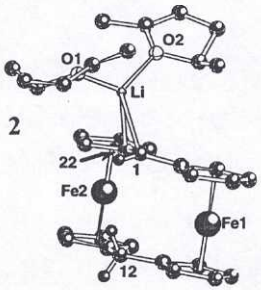

UV-vis spectroscopic studies show that **2** exists predominantly as a contact ion pair (CIP) in the temperature range -100 °C to +25 °C in tetrahydrofuran (THF), 2,5-dimethyltetrahydrofuran (DMTHF) and diethyl ether (DEE). In dimethoxyethane (DME) **2** exists mainly as a CIP above +25 °C, but below -30 °C mainly as a solvent separated ion pair (SSIP).

The initial state of **2** have been shown to be monomeric in DMTHF, based on ^{13}C-^{6}Li coupling pattern.

It has been possible to crystallise **2** in DMTHF and determine the structure. This novel structure showed that lithium is located in an *exo*-position coordinated to two solvent molecules, C_1 and C_{22}. Compound **2** is a monomer in the solid state as well. In contrast to earlier reports, based on ^{1}H NMR studies, which suggested an intramolecular $C_1^-\cdots H\text{-}C_{12}$ hydrogen bond, no such interaction is present in the solid state.

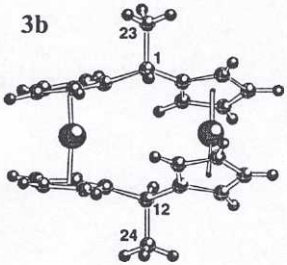

The detailed role of the solvent in the intramolecular 1,12-lithiation in **2** has been elucidated by dynamic NMR spectroscopy. The reaction is about 4000 times faster in THF than in DMTHF. Thus, it has been possible to catalyse the reaction by THF in DMTHF. The catalysis is first order in THF at low concentrations, which shows that the rate limiting transition state contains one solvent molecule more than the initial state.

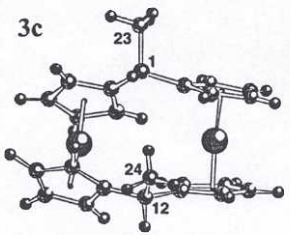

The precursor of **2**, *i.e.* [1.1]ferrocenophane (**1**), undergoes a fast degenerate conformational rearrangement. Dynamic NMR studies gave the Gibbs free energy of activation (28 ± 4 kJ mol^{-1}) for this process. The mechanism has been concluded to be either a pseudo-rotation or a ring-inversion, similar to that found for cyclohexane.

Two novel isomers of the 1,12-dimethyl derivative of **1**, *i.e.* 1,12-dimethyl-[1.1]ferrocenophane (**3**) have been crystallised and structurally characterised by X-ray diffraction methods. One is the first carbon-bridged anti[1.1]ferrocenophane, *i.e.* *exo,exo,anti*-1,12-dimethyl-[1.1]-ferrocenophane (**3b**), a type of isomer that has previously been ruled out due to steric strain. The other isomer is *exo,endo,syn*-1,12-dimethyl-[1.1]ferrocenophane (**3c**). These isomers show a conformational behaviour that is similar to that of 1,4-dimethylcyclohexane.

Keywords: [1.1]ferrocenophanyllithium, alkali metallation reactions, solvent catalysis, structure, mechanism, ^{13}C-^{6}Li coupling, dynamic NMR, X-ray, UV-vis, [1.1]ferrocenophane, pseudo-rotation, ring-inversion, conformational analysis, isotopic labelling.

ISBN: 91-7197-088-6

Investigations of structure and dynamics of [1.1]ferrocenophanes and their alkali metal salts

Unravelling of the detailed mechanism of an alkali metallation reaction and the conformational properties of [1.1]ferrocenophanes by NMR-, UV-vis-spectroscopy and X-ray diffraction

by

Jan-Martin Löwendahl

A dissertation submitted in partial fulfilment
of the requirements for the degree of
Doctor of Philosophy in Chemistry

Department of Organic Chemistry
Göteborg University
Göteborg, Sweden
1995

"Vad kan jag överhuvudtaget veta?"
René Descartes, 1596-1650.

ISBN 91-7197-088-6
Göteborg 1995

ABSTRACT

Insight into the detailed mechanism of alkali metallation reactions has been obtained using 1-[1.1]ferrocenophanyllithium (**2**) and the corresponding sodium, potassium and cesium salts. These compounds undergo fast degenerate intramolecular 1,12-carbon metallation. The importance of aggregation, ion pairing, gegenion, solvation and to some extent the carbanion have been studied.

UV-vis spectroscopic studies show that **2** exists predominantly as a contact ion pair (CIP) in the temperature range -100 °C to +25 °C in tetrahydrofuran (THF), 2,5-dimethyltetrahydrofuran (DMTHF) and diethyl ether (DEE). In dimethoxyethane (DME) **2** exists mainly as a CIP above +25 °C, but below -30 °C mainly as a solvent separated ion pair (SSIP).

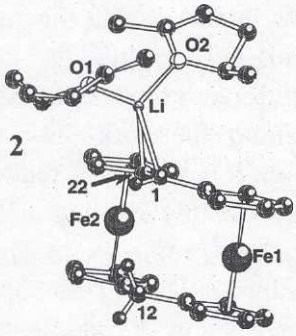

The initial state of **2** have been shown to be monomeric in DMTHF, based on ^{13}C-^{6}Li coupling pattern.

It has been possible to crystallise **2** in DMTHF and determine the structure. This novel structure showed that lithium is located in an *exo*-position coordinated to two solvent molecules, C_1 and C_{22}. Compound **2** is a monomer in the solid state as well. In contrast to earlier reports, based on ^{1}H NMR studies, which suggested an intramolecular $C_1^-\cdots H\text{-}C_{12}$ hydrogen bond, no such interaction is present in the solid state.

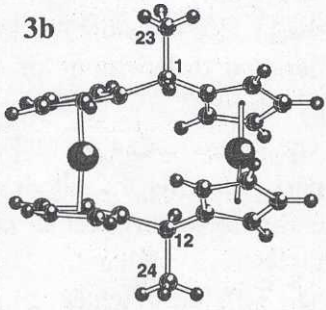

The detailed role of the solvent in the intramolecular 1,12-lithiation in **2** has been elucidated by dynamic NMR spectroscopy. The reaction is about 4000 times faster in THF than in DMTHF. Thus, it has been possible to catalyse the reaction by THF in DMTHF. The catalysis is first order in THF at low concentrations, which shows that the rate limiting transition state contains one solvent molecule more than the initial state.

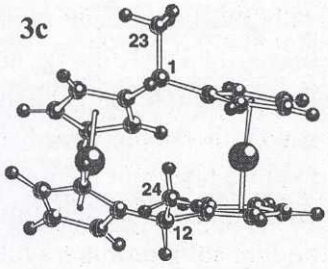

The precursor of **2**, *i.e.* [1.1]ferrocenophane (**1**), undergoes a fast degenerate conformational rearrangement. Dynamic NMR studies gave the Gibbs free energy of activation (28 ± 4 kJ mol^{-1}) for this process. The mechanism has been concluded to be either a pseudo-rotation or a ring-inversion, similar to that found for cyclohexane.

Two novel isomers of the 1,12-dimethyl derivative of **1**, *i.e.* 1,12-dimethyl-[1.1]ferrocenophane (**3**) have been crystallised and structurally characterised by X-ray diffraction methods. One is the first carbon-bridged anti[1.1]ferrocenophane, *i.e.* *exo,exo,anti*-1,12-dimethyl-[1.1]-ferrocenophane (**3b**), a type of isomer that has previously been ruled out due to steric strain. The other isomer is *exo,endo,syn*-1,12-dimethyl-[1.1]ferrocenophane (**3c**). These isomers show a conformational behaviour that is similar to that of 1,4-dimethylcyclohexane.

Keywords: [1.1]ferrocenophanyllithium, alkali metallation reactions, solvent catalysis, structure, mechanism, ^{13}C-^{6}Li coupling, dynamic NMR, X-ray, UV-vis, [1.1]ferrocenophane, pseudo-rotation, ring-inversion, conformational analysis, isotopic labelling.

Preface and acknowledgements

This thesis is in general based on the Papers I through VII which are listed on page IV.

My intention with this thesis, is to present the knowledge that has been gathered about the [1.1]ferrocenophane systems, so far. I will start with "Introduction and summary" which is a short account of the motivation behind this work and a summary of the conclusions that can be made from this work. Thereafter, there will be two background sections. The first mainly dealing with the history of alkali metallation reactions leading to our work. The second will more specifically deal with the history of [1.1]ferrocenophanes and their structures.

The section "Experimental" contains a rather short presentation of some of the different methods that have been used to gather information about the [1.1]ferrocenophane system. Furthermore, this section contains more detailed descriptions of some experimental procedures that we have developed.

The section "Results and discussion" is divided into two parts. The first part concerns the alkali metallation reaction in [1.1]ferrocenophanyl carbanions. The second part presents the conformational studies of the [1.1]ferrocenophanes.

The articles on which the main part of this thesis is built, are collected at the end of this thesis.

This work has been done by a group of people under the guidance of professor Per Ahlberg, and what I will do, is to present the information that I find relevant. When doing this, I will of course put an emphasis on my part of the work, since this is my thesis. However, I will already here express my gratitude towards my fellow group members: our "Benjamin", Annika Karlsson, for companionship and for fruitful discussions, she will undoubtedly produce a lot of results with her hardworking attitude, Göran Hilmersson my present roommate for his friendship and for *enthusiastic* and fruitful discussions and special thanks to Dr. Öjvind Davidsson, the first to enter into this area and therefore the one who had to take the first knocks when developing techniques and "getting to know our molecules". He has been a very good friend during these years. Last, but by no means least, I would like to thank my supervisor professor Per Ahlberg, a true scientist, who has been an excellent guide in **all** aspects of the academic

world, everything from critical analysis of experimental results to how to get your opinion through in the boardroom.

I would like to end this preface with acknowledgements.

During my years at the department, working with this project, I have come to meet so many friendly and helpful people that it will take quite a few lines to thank only some of them.

Lars Baltzer for his expert NMR advice. Hans Svensson, our skilled technician. Kerstin Bohman, our secretary without whom the department would crumble. Reine Torberntsson, our helpful engineer. Sven Thulin and Nils Holgersson for their excellent glasswork. Thomas Olsson for sharing his vast knowledge about computers, chemistry, balloon flying... Oskar Axelsson for many interesting discussions and just being a friend. Peder Svensson, Tommy Iliefski and Björn Sandell, all brothers in arms on the battle field of increasing computerisation. Mikael Håkansson for his work at the diffractometer and his scientifically correct sceptical attitude towards new experiments. Dieter Cremer, Lars Olsson and Henrik Ottosson for many fruitful discussion mostly regarding ferrocenophanes and *ab initio* calculations (and for finally carrying out some calculations). Staffan Schantz for helping out with solid state NMR. Gideon Fraenkel and his family for their hospitality. Albert Chow for his special friendship, I hope we will meet again. Dr. Derek Biddle for linguistic improvements of this manuscript. All my other friends at the departments, both at Göteborg University and at Chalmers University of Technology.

All the people I have met in the student organisation and the labour union for giving me insight into the world of other faculties and helping me understand the bureaucratic side of academia.

All the acquaintances I have made being the network manager in the chemistry building for giving me yet another perspective of the academic world.

And, of course, Christina, my sambo, for her love, support and patience.

List of articles

This thesis is based on the Papers I through VII. These articles are collected at the end of this thesis.

I. Monomeric 'Benzyl Lithium' in 2,5-Dimethyltetrahydrofuran. NMR Spectroscopic Studies of ^{6}Li and $^{13}C_2$ Labelled Ferrocenophanyl Lithium using ^{13}C-^{6}Li Coupling and ^{6}Li Decoupling

Öjvind Davidsson, Martin Löwendahl and Per Ahlberg.

J. Chem. Soc., Chem. Commun. **1992**, 1004-1005.

II. Crystal Structure of Ferrocenophanyllithium: Absence of an Intramolecular C-H...-C Hydrogen Bond

Per Ahlberg, Öjvind Davidsson, Göran Hilmersson, Martin Löwendahl and Mikael Håkansson.

J. Chem. Soc., Chem. Commun. **1994**, 1573-1574.

III. Catalysis of an Alkali metallation Reaction - Mechanistic Studies of the Intramolecular Degenerate Rearrangement of [1.1]ferrocenophanyllithium.

Öjvind Davidsson, Martin Löwendahl, Göran Hilmersson and Per Ahlberg.

J. Am. Chem. Soc., submitted for publication.

IV. Pseudorotation in [1.1](1.1')Ferrocenophane, a Molecular Acrobat: a Study by Dynamic ^{1}H Nuclear Magnetic Resonance Spectroscopy

Martin Löwendahl Öjvind Davidsson and Per Ahlberg.

J. Chem. Research (S) **1993**, *1*, 40-41.

V. A *syn*-[1.1]Ferrocenophane with Approximate C_{2v} Symmetry

Mikael Håkansson, Martin Löwendahl, Öjvind Davidsson and Per Ahlberg.

Organometallics **1993**, *12*, 2841-2844.

VI. First Evidence for a Carbon-Bridged [1.1]Ferrocenophane in the *anti* Conformation. Molecular Structure of *exo,exo,anti*-1,12-Dimethyl[1.1]ferrocenophane

Martin Löwendahl, Öjvind Davidsson, Per Ahlberg, and Mikael Håkansson.

Organometallics **1993**, *12*, 2417-2419.

VII. 1,12-Dimethyl[1.1]ferrocenophane - an Organometallic Cyclohexane Analogue with Extraordinary Flexibility. Molecular Structure of a Third Isomer: *exo,endo,syn*-1,12-Dimethyl[1.1]ferrocenophane.

Jan-Martin Löwendahl and Mikael Håkansson.

Organometallics, submitted for publication.

Molecular structures

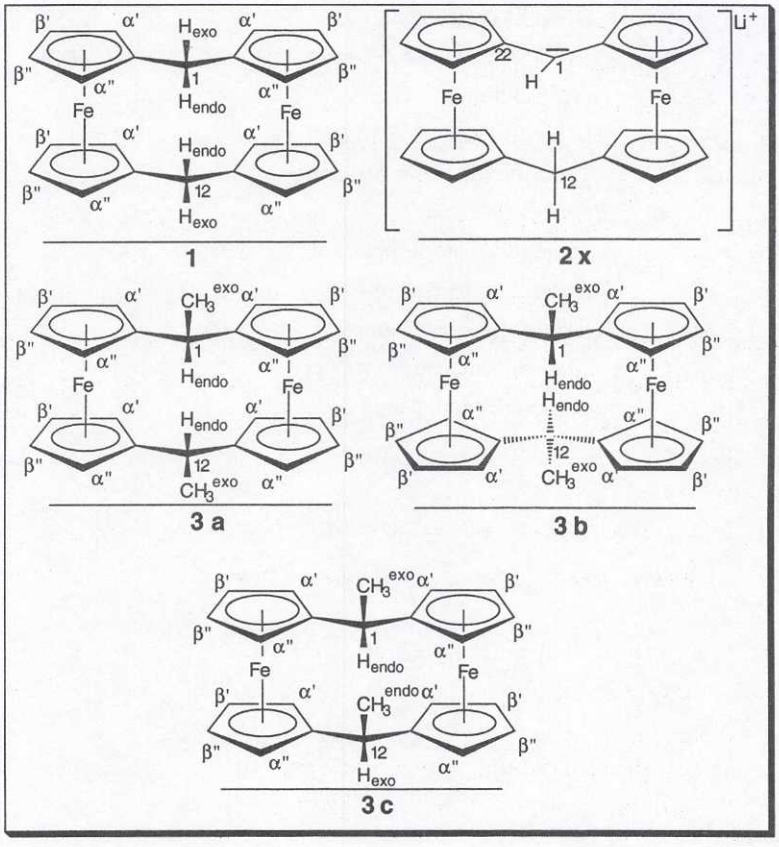

Abbreviations

THF	Tetrahydrofuran
DEE	Diethyl ether
DMTHF	Dimethyltetrahydrofuran
THP	Tetrahydropyran
MTHF	2-Methyl-tetrahydrofuran
DME	Dimethoxyethane
DMPU	1,3-dimethyl-3,4,5,6-tetrahydro-2(1H)-pyrimidinone
n-BuLi	n-Butyllithium
MeLi	Methyllithium
TMEDA	Tetra-methyl-ethylenediamine
FCP	Ferrocenophane
DMFCP	Dimethylferrocenophane
CIP	Contact Ionpair
SSIP	Solvent Separated Ionpair
NMR	Nuclear Magnetic Resonance
UV-vis	Ultraviolet and visible

Contents

1 Introduction and summary

1.1 Introduction

An article in C&EN, "Ferrocene derivatives exhibit unusual chemistry", sparked our interest in [1.1]ferrocenophanes.[1] This article was based on the work of Mueller-Westerhoff and coworkers,[2] who claimed "the first verified C-H-C hydrogen bond". This observation was made with a compound that was made from [1.1]ferrocenophane (**1**), Figure 1.1, and n-butyllithium (n-BuLi) in tetrahydrofuran (THF), Figure 1.2.

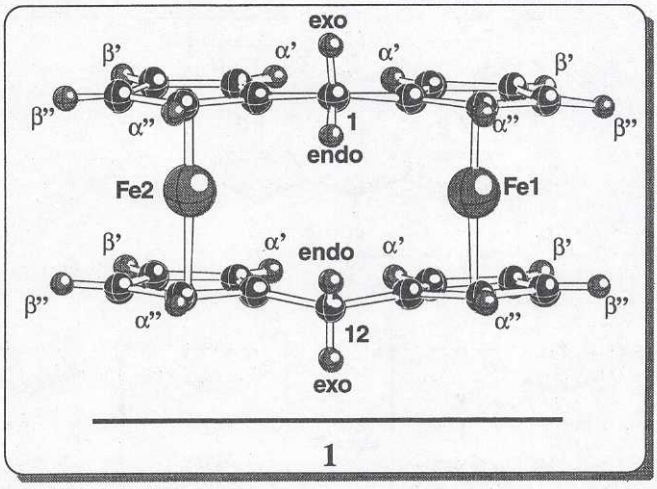

Figure 1.1. [1.1]ferrocenophane (**1**) consists of two ferrocene units connected with two bridges consisting of one methylene unit each.

The result of this intermolecular lithiation reaction was metallation of one of the methylene carbons in **1**, *i.e.* 1-[1.1]ferrocenophanyllithium (**2**) is formed.

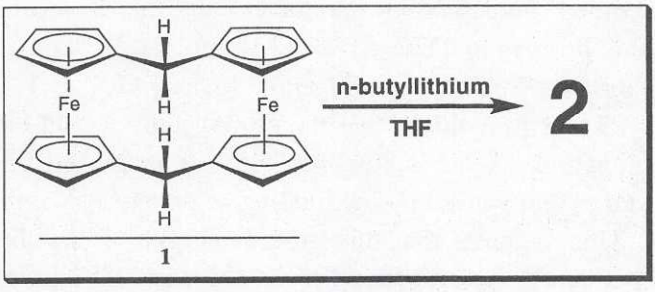

Figure 1.2. The reaction of **1** with n-BuLi in THF forming **2**.

From NMR studies of **2** and related compounds, Mueller-Westerhoff and coworkers claimed to have found evidence for the first intramolecular $[C\text{-}H\text{-}C]^-$ hydrogen bond. Their findings were consistent with an initial

state (IS) for **2** being either the form with a symmetric hydrogen bond [C···H···C]⁻ (**2a**), or a form with an asymmetric hydrogen bond [C-H···C]⁻ (**2b**), in which the *endo* proton is rapidly jumping between carbons 1 and 12 (Figure 1.3).

Ahlberg and coworkers, being interested in hydrogen bonded carbanions,[3] decided to resolve this problem. Ahlberg and Davidsson proved that **2** undergoes a degenerate intramolecular proton transfer (Figure 1.3b).[4] These results obtained with dynamic NMR spectroscopy, were consistent with **2b** being the initial state form.

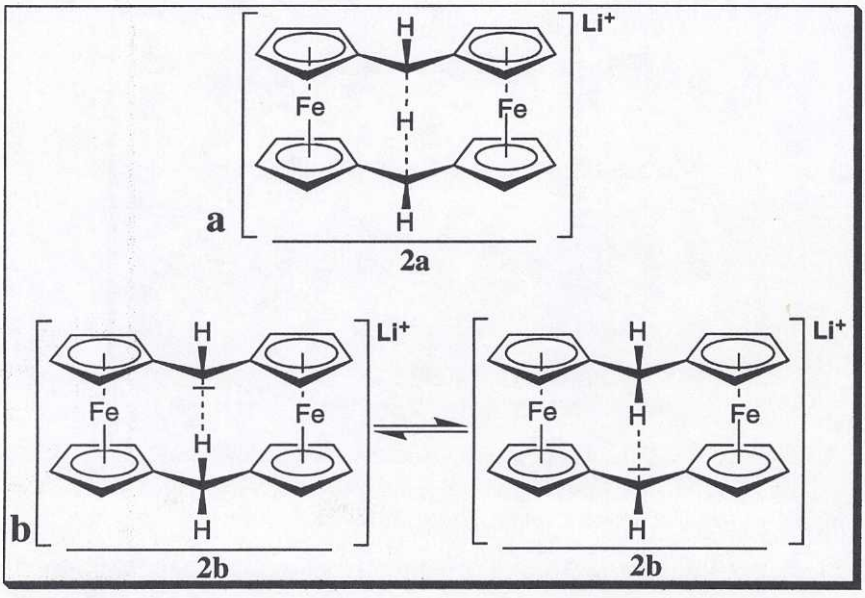

Figure 1.3. a) The static form of **2** (**2a**). b) The dynamic form of **2** (**2b**).

They determined the activation parameters and the deuterium isotopic effect for this process in THF: $\Delta G^{\ddagger}$= 42 kJ mol^{-1} (-24 °C), $\Delta H^{\ddagger}$= 19 kJ mol^{-1} and $\Delta S^{\ddagger}$= -93 J K^{-1} mol^{-1} and k_H/k_D= 7.4 ± 1.5 (47 °C) respectively. The k_H/k_D shows that the proton jump is rate limiting and the large negative $\Delta S^{\ddagger}$ indicates that there is increased order in the transition state (TS), caused by the binding of an extra solvent molecule to lithium. This suggests that this process (Figure 1.3b) should show solvent dependence. This is found to be the case. The intramolecular proton jump in **2** is 4000 times faster in THF than in 2,5-dimethyltetrahydrofuran (DMTHF).[5] Furthermore, the rate constant for the proton jump is concentration independent. This suggests that lithium,

also moves intramolecularly, *i.e.* the reaction in **2** is a degenerate intramolecular lithiation reaction.

The lithiation reaction in **2** is thus an example of alkali metallation reactions (Figure 1.4).

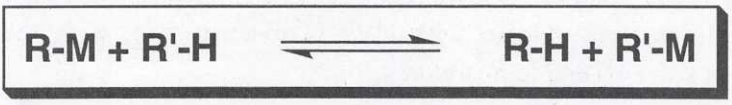

Figure 1.4. A general definition of an alkali metallation reaction.

One of the most encountered reactions in this class is when an alkyllithium (R-M) as the base reacts with a carbon acid (R'-H) to produce the corresponding alkane (R-H) and a reactive intermediate (R'-M). This intermediate is then converted into the product by electrophilic substitution at the carbanionic carbon. This reaction has become very useful in synthetic chemistry, especially since n-butyllithium became commercially available in the early 1960's.

Despite the usefulness of organo alkali metal chemistry, there are few detailed mechanistic investigations in this important field. However, the interest has been growing rapidly the last two decades. Why is this the case? Well, there are many problems involved when studying this type of reactions. It is in the very nature of organo alkali metal reagents, like n-butyllithium, to be very reactive, *i.e.* they react rapidly with a wide range of compounds, including water. This means that extremely controlled conditions (like inert and moisture free atmosphere) are needed. Furthermore, the method of observation must be sufficiently fast in order to obtain the kinetic information needed for mechanistic interpretations.

One solution to these problems is to find a system in which the alkali metallation reaction is degenerate. This is exactly the case with **2**, which is conveniently studied by dynamic NMR spectroscopy. Thus -

The [1.1]ferrocenophanyl carbanions are excellent probes for investigating the mechanism of alkali metallation reactions.

What kind of information do we seek? First of all, for the elucidation of the detailed mechanism of alkali metallation reactions it is necessary to have knowledge about both the initial state (IS) and the transition state (TS). Furthermore, earlier investigations have established that important factors in alkali metallation reactions are: the *gegenion*, the *ion-pairing*, the *aggregation* state, the *structure of the carbanion* and the *solvent*.

1.2 Summary

1.2.1 Alkali metallation

The ion-pairing equilibrium (Figure 1.5) between solvent separated ionpair (SSIP) and contact ionpair (CIP) of [1.1]ferrocenophanyl alkali metals have been studied with UV-vis spectroscopy, with respect to different solvents and temperatures.

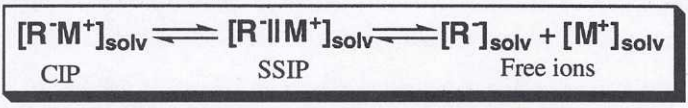

Figure 1.5. The equilibrium between CIP, SSIP and free ions.

The initial state of **2** in THF, DMTHF and diethyl ether (DEE) is mainly made up of CIPs in the temperature range, +25 °C to -100 °C. In dimethoxyethane (DME) there are mainly CIPs at +25 °C and mainly SSIPs below -30 °C and possibly even free ions at lower temperatures. The effect of the change in ionpairing equilibrium is that the rate of the intramolecular lithiation reaction in **2** in DME is similar to that in THF at +25 °C, but at lower temperatures the rate is higher in DME than in THF.

Knowledge of the aggregation state is crucial since the reactivity of an alkali metallated compound is dependent on this (Figure 1.6).

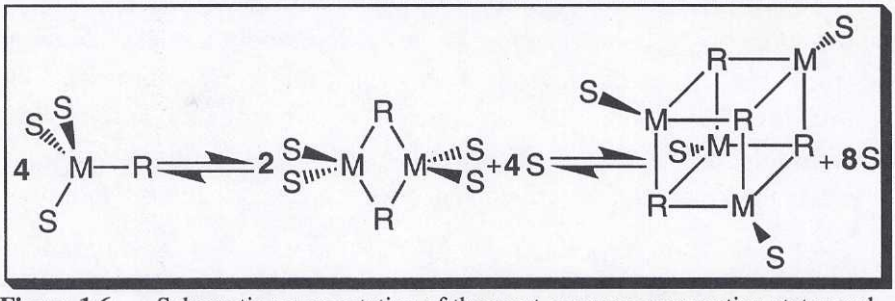

Figure 1.6. Schematic representation of the most common aggregation states and their equilibrium.

The ^{13}C-^{6}Li coupling pattern studied by ^{13}C NMR spectroscopy can give information about the aggregation state of organolithium compounds. The isotopically labelled compound [1-^{6}Li]-[1,12-$^{13}C_2$]-[1.1]ferrocenophanyllithium (**^{13}C-^{6}Li-2**) made from [1,12-$^{13}C_2$]-[1.1]ferrocenophane and [1-^{6}Li]-n-butyllithium, was studied with multinuclear 1D NMR spectroscopy. In the ^{13}C NMR spectrum of **^{13}C-^{6}Li-2** in DMTHF, the signal from the carbanionic carbon appeared as a 1:1:1 triplet due to ^{6}Li coupling (^{6}Li is a spin 1 nucleus). This proves that the initial state of **2** is

monomeric in DMTHF solution and that the lithium ion is coordinated to the carbanionic bridge carbon (Paper I).

We have succeeded in crystallising **2** in DMTHF and in determining the structure (Paper II). This novel structure (Figure 1.7) showed that lithium is located in an *exo* position coordinated to two solvent molecules, C_1 and C_{22} (tetra-coordination). Compound **2** is a *monomer* in the solid state as well. The carbanionic carbon has an hybridisation of about $sp^{2.5}$. Furthermore, in contrast to earlier reports (*vide infra*), which suggested an intramolecular $C_1^-\cdots H\text{-}C_{12}$ hydrogen bond, we found no such bond in the solid state.

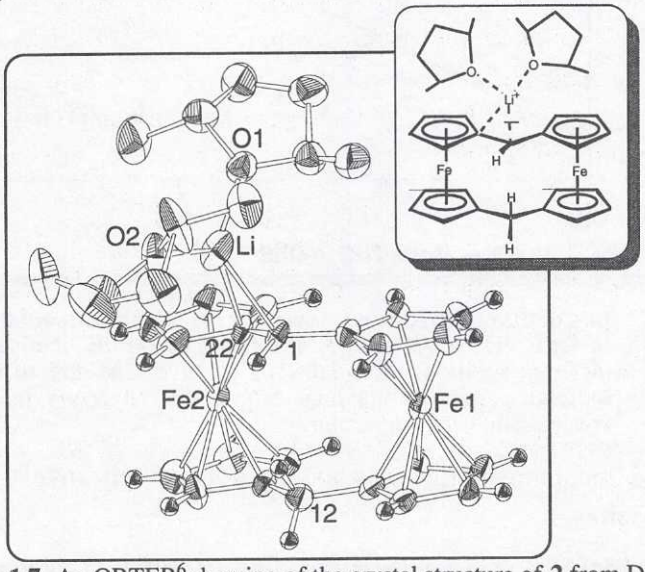

Figure 1.7. An ORTEP[6] drawing of the crystal structure of **2** from DMTHF.

The intramolecular proton jump in **2** is 4000 times faster in THF than in DMTHF or DEE.[5] This large rate difference makes it possible to catalyse this reaction in *e.g.* DEE by small amounts of THF or DME (Figure 1.8). The catalysis is first order in THF at low concentrations, this shows that the rate limiting transition state contains one solvent molecule more than the initial state (Paper III).

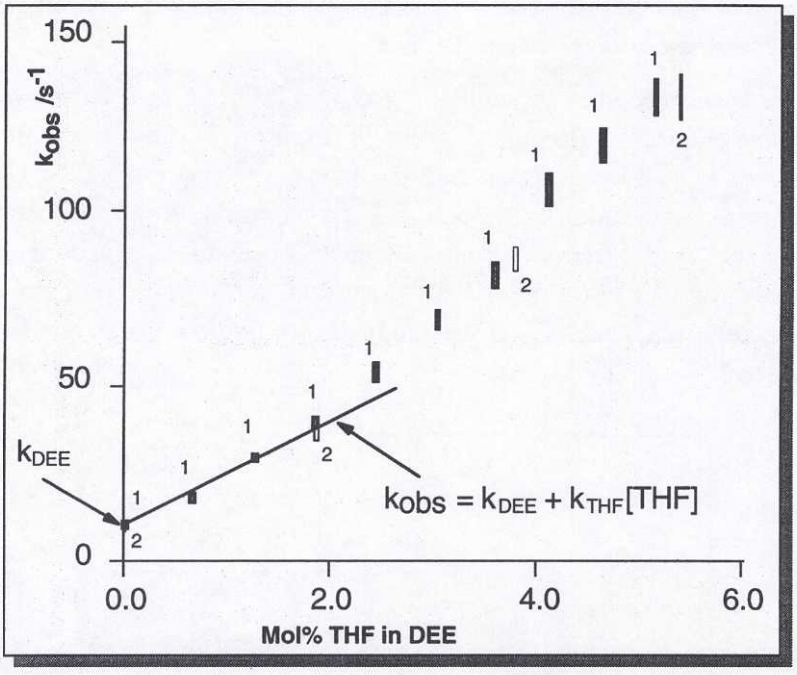

Figure 1.8. Plot of the observed rate constant for the intramolecular lithiation of **2** in DEE versus the mol % of THF. The results obtained with two different solutions of **2**, labelled 1 and 2. The size of the markers indicate estimated maximal errors, due to errors in rates, THF concentration and temperature.

A detailed mechanism that has emerged from our investigations is presented below.

1. In the initial state **2** is a monomer and a CIP with two solvent molecules ligated to the lithium ion (A in Figure 1.9)
2. From A, an intermediate is formed with an extra solvent molecule ligated to the lithium, thereby increasing the $C_1^-\cdots Li^+$ distance (B).
3. In the alkali metallation TS, the proton is in the middle of the carbons 1 and 12 (C).
4. The intermediate is reformed with the carbanionic carbon being C_{12}^- and where the lithium ion and proton have moved to the opposite carbon bridge, respectively (D).
5. The intermediate loses the third solvent molecule and the initial state is reached again (E).

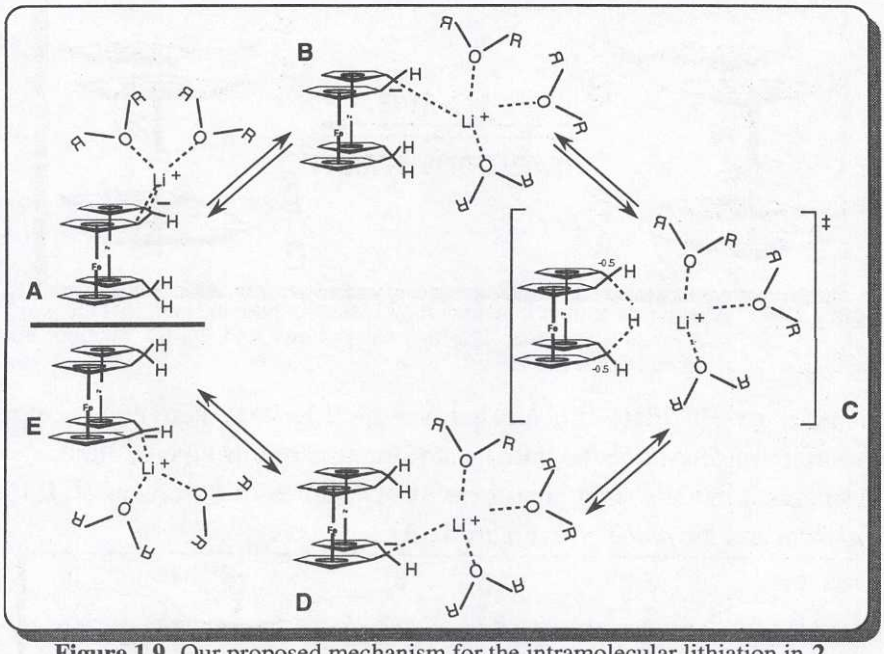

Figure 1.9. Our proposed mechanism for the intramolecular lithiation in **2**.

1.2.2 Conformational studies of [1.1]ferrocenophanes

Despite the complexity of **1**, the ^{1}H NMR spectrum of **1** consists of only three signals. This could be the result of accidental chemical shift equivalence. However, already in 1967 Watts suggested, with the aid of Dreiding models, that a complicated degenerate internal inter conversion was responsible for the low number of signals (Figure 1.10).[7] Neither Watts nor Mueller-Westerhoff, the major figures in [1.1]ferrocenophane chemistry, could prove that an internal degenerate motion was responsible for the simple NMR spectrum. We have been able, using new technique (highfield NMR spectroscopy and a solvent mixture of THF and DEE [1:1, v/v]), to freeze out an internal motion and determine the Gibbs free energy of activation to be 28 ± 4 kJ mol^{-1} (Paper IV).

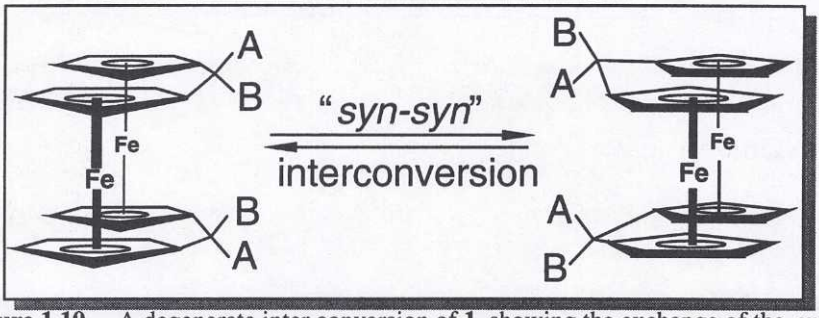

Figure 1.10. A degenerate inter conversion of **1**, showing the exchange of the *exo* and *endo* positions. The α', α" protons and β', β" protons also exchange simultaneously.

In order to elucidate the mechanism of this inter conversion, it is important to determine the initial state structure of this type of molecules. Mechanical models show that there exist two possible isomers of **1**; the *syn*-form and the *anti*-form (Figure 1.11).

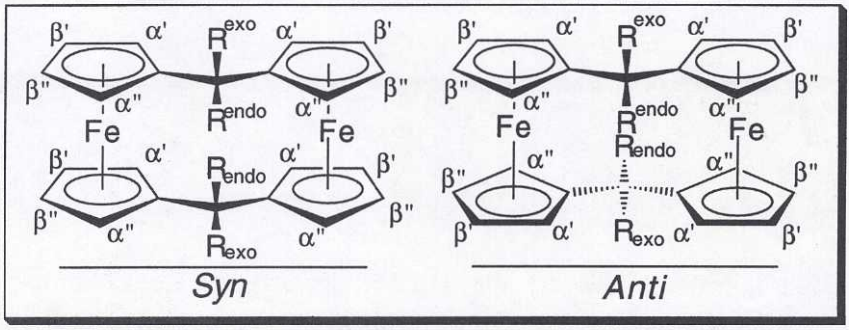

Figure 1.11. *Syn* and *anti* conformers of [1.1]ferrocenophanes with *exo*, *endo* and ring positions marked.

The first lead regarding this question came when an isomer of the dimethyl derivative of **1** , *i.e.* 1,12-dimethyl-[1.1]ferrocenophane (DMFCP), was crystallised and structurally characterised by X-ray diffraction. This isomer proved to be *exo,exo,syn*-1,12-dimethyl-[1.1]ferrocenophane (**3a**) (Figure 1.12).[8,9] This experimental result and investigations of molecular models led Watts to believe that the flexible *syn*-conformer, and not the rigid and sterically crowded *anti*-conformer, was the preferred structure of [1.1]ferrocenophanes. Especially since the flexibility of the *syn*-conformer easily allows such an isomer to twist in order to relieve the steric repulsion between the α' protons. These considerations led to the exclusion of *anti*-conformers as stable compounds. A second isomer, isolated from the synthesis of DMFCP, was assigned an *exo,endo,syn* structure[10,11] using NMR spectroscopy. It was recognised that in order for the assignment to be valid, a similar

degenerate internal motion that is taking place in **1** had also to take place in the *exo,exo,syn*-isomer, since the NMR spectrum is simpler than the structure of this conformer implies.

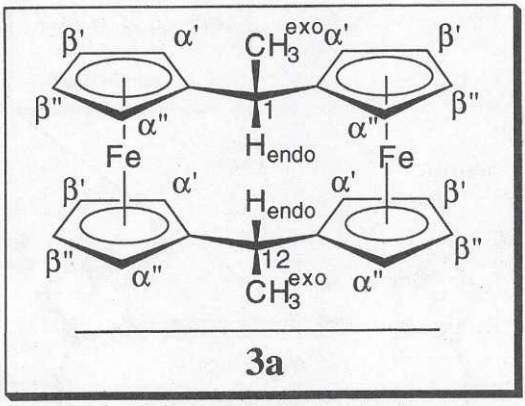

Figure 1.12. Isomer **3a**, which for simplicity is shown as a C_{2v} symmetry conformation rather than in the twisted C_2 symmetry conformer found in the solid state structure.

When we performed the synthesis of DMFCP, we managed to produce four different types of crystals. Two of them were crystallised from a solution of DMFCP in hexane. These, orange-red cubes and orange-red needles, were separated by hand and their structures determined by X-ray diffraction. The cubic crystals consisted of the previously characterised **3a**. The needle like crystals also consisted of **3a**, but the packing was different. This phase was non-centrosymmetric and the crystals showed optical activity.

Chirality can be induced in a [1.1]ferrocenophane type molecule, by *the twist* (section 5.2.4). One enantiomer is formed upon twisting the right ferrocene unit upward and the other isomer is formed upon twisting the left ferrocene unit upward (Figure 1.13).

This type of motion in *e.g.* **1**, has a C_{2v} type TS which renders chemical shift equivalence to the α', α", β' and β" protons respectively, but not between *exo*- and *endo*-, α'- and α"- and β'- and β"-protons. Interestingly enough, **1** crystallises in two forms. One twisted form (**1a**, twist angle = 13°) that has been reported by Mueller-Westerhoff and coworkers[12] and one C_{2v} like form (**1b**) with a twist angle of 3° (Figure 1.14) (Paper V).

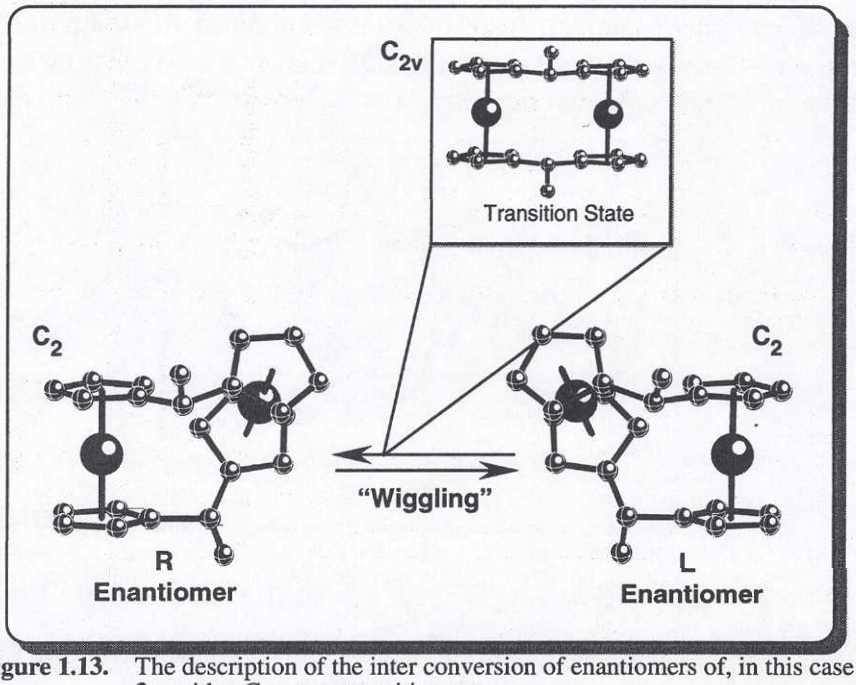

Figure 1.13. The description of the inter conversion of enantiomers of, in this case **3a**, with a C_{2v} type transition state.

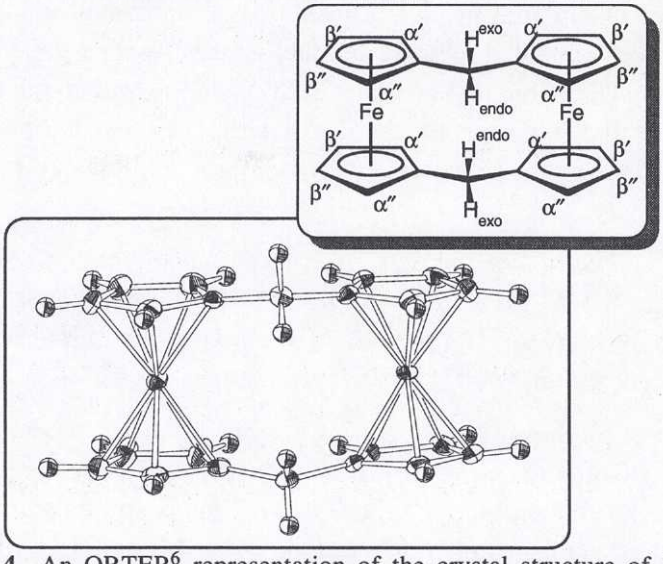

Figure 1.14. An ORTEP[6] representation of the crystal structure of **1b** with a diagrammatical representation in the upper right corner

Immediate rinsing of the crystals of **3a** with hexane gave a solution from which a third type of crystals was obtained. To our surprise, these deeply red rhombic crystals turned out to consist of the first carbon bridged *anti*-[1.1]ferrocenophane, *i.e. exo,exo,anti*-1,12-dimethyl-[1.1]ferrocenophane

(**3b**) (Paper VI). This *anti*-isomer with its tilted ferrocene unit is shown in Figure 1.15.

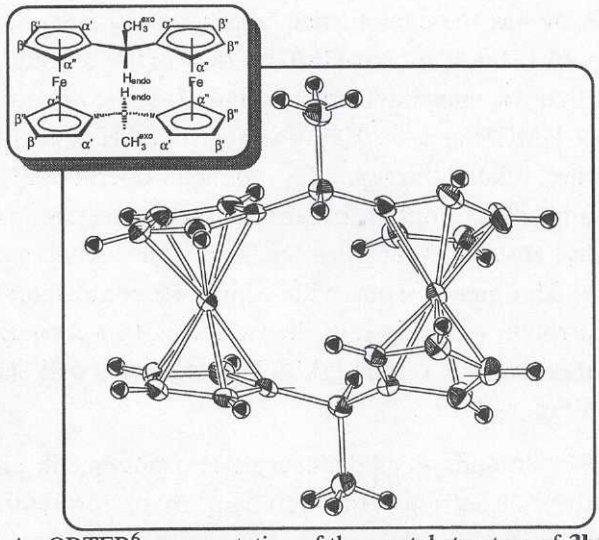

Figure 1.15. An ORTEP[6] representation of the crystal structure of **3b** with a diagrammatical representation in the upper left corner

Later, a fourth type of crystals was obtained from THF. It was deeply red needle shaped crystals of what was found to be a third isomer of DMFCP, *i.e. exo,endo,syn*-1,12-dimethyl-[1.1]ferrocenophane (**3c**) (Figure 1.16) (Paper VII).

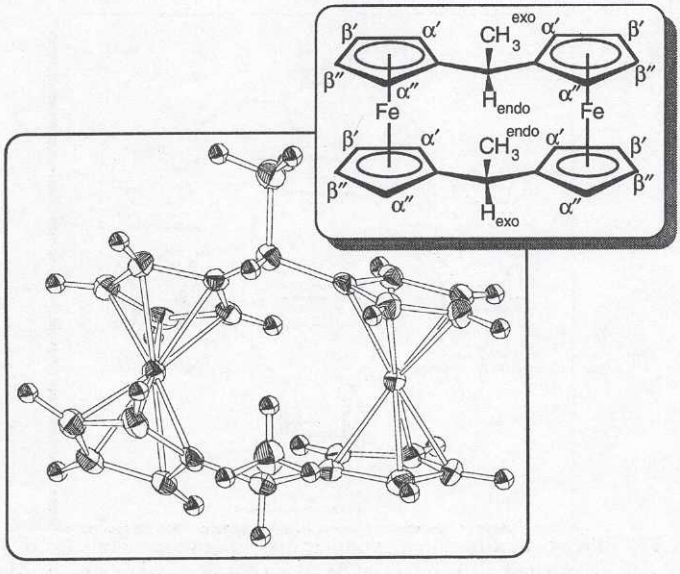

Figure 1.16. An ORTEP[6] representation of the crystal structure of **3c** with a diagrammatical representation in the upper right corner

There is an interesting analogy between the [1.1]ferrocenophane system and the cyclohexane system.

For example, **3c** has the cyclohexane analogue 1(a),4(e)-boat-dimethyl-cyclohexane **4a** (1(a),4(e)-boat-DMCH) (a = axial, e = equatorial). It is well known that **4a** may inter convert into 1(e),4(a)-boat-DMCH. The 1(a),4(e)-boat-DMCH and the 1(e),4(a)-boat-DMCH isomers are actually the same isomer, related through a C_2 symmetry operation, *i.e.* the methyl groups exchange. This implies that if this inter conversion is sufficiently fast, the methyl groups would show up as only one signal in *e.g.* ^{1}H NMR spectroscopy. The mechanisms with which **4a** could inter convert, are either pseudo-rotation or ring-inversion via 1(e),4(e)-chair-DMCH **4b**. If we projects this scenario on the DMFCP system, we will end up in what is depicted in Figure 1.17.

In Figure 1.17, **3c** undergoes degenerate rearrangement, either through pseudo-rotation directly or through ring-inversion with **3b** as an intermediate.

The fact that the solution spectrum of dissolved crystals of **3b** is identical with that of dissolved crystals of **3c**, indicates the presence of a ring-inversion pathway. Dynamic NMR studies of the isomeric mixture of 1,12-([23,24-$^{13}C_2$]-dimethyl)-[1.1]ferrocenophane (**^{13}C-3**) indicate the presence of a fast rearrangement.

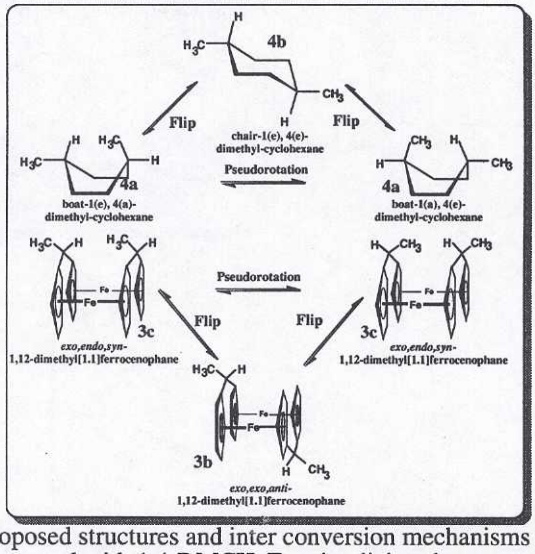

Figure 1.17. Proposed structures and inter conversion mechanisms of **3c** and **3b**, compared with 1,4-DMCH. For simplicity, the comparison is made between boat and *syn*-structures and chair and *anti*-structures rather than their energetically more likely twisted forms.

2 Alkali metallation - background

This section shortly describes the evolution of alkali metallation chemistry, an important part of organometallic chemistry. Furthermore, some important factors concerning the nature of alkali organometallic reagents are presented.

2.1 History and significance

A hundred years after the discovery of the lightest metal, lithium, in 1817 by J. A. Arfvedsson (pupil of J. J. Berzelius),[13] W. Schlenk published the preparation of alkyllithiums, *i.e.* methyllithium, ethyllithium and phenyllithium via transalkylations of mercury organometallic derivatives (Figure 2.1).[14] However, it was not until 1928 that he reported a reaction using these alkyllithiums the way we use them today, *i.e.* the lithiation of fluorene with ethyllithium[22] (Figure 2.2).

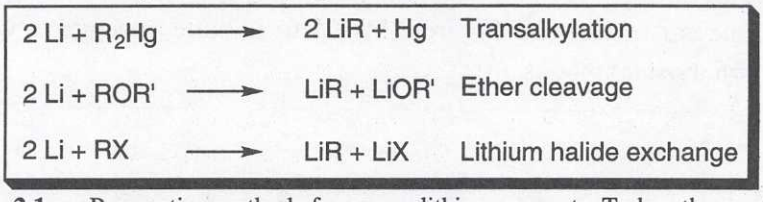

Figure 2.1. Preparative methods for organolithium reagents. Today, the most used method is lithium halide exchange.

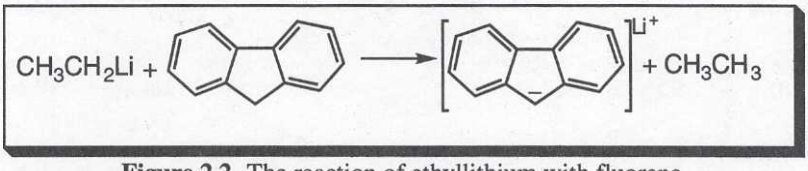

Figure 2.2. The reaction of ethyllithium with fluorene.

Before the extensive use of organolithium compounds in synthesis could evolve, improvements in the handling and preparation of alkyllithiums were necessary (Figure 2.1). Many chemists were involved in this process which started during the 1930's. Important contributions were made by; K. Ziegler, [15] G. Wittig[16] and H. Gilman,[17,18] who developed and demonstrated the synthetic use of alkyllithiums.

The synthetic usefulness is increasing steadily and is currently focused on enantioselective synthesis with the aid of chiral ligands.
The introduction and rapid development of techniques such as NMR spectroscopy, X-ray diffraction analysis and *ab initio* calculations, have

gradually increased the amount and depth of mechanistic investigations in this field. Over the years, investigations have shown that the nature of organometallic reagents depend on the gegenions, ionpairing, aggregation, solvent and the structure of the carbanion.

2.2 Gegenions - their role

When considering gegenion effects in organo alkali metallic compounds (RM, M=Li, Na, K, Rb, Cs), one distinguishes between two different types of species: type I, those with σ-donor substituents (typically R = CH_3) and type II, species with σ- and π-donor substituents (typically R = cyclopentadienyl).[19]

The nature of the carbon-metal bond has been disputed for years, but it is now generally agreed that these bonds are highly ionic with only a small covalent contribution even in the type I compounds. The type I species are specially interesting since the alkali metals in these compounds show a nonmonotonous trend in electronegativity with Li being less electronegative than Na (Figure 2.3).[20] This is quite opposite to what is taught in most textbooks.

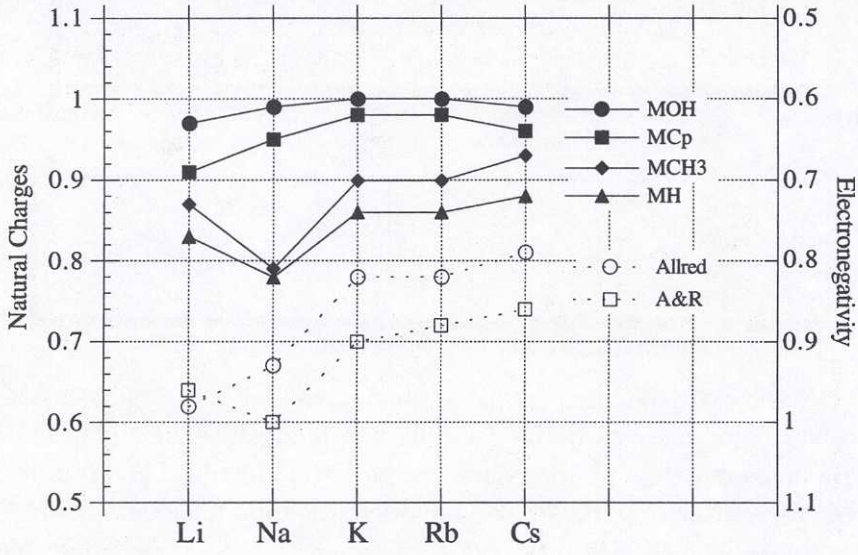

Figure 2.3. Natural charges on the metal calculated at the Hartree-Fock level (left scale) for the RM compounds (R = CH_3, H, Cp, OH) as well as Allred and Allred-Rochow electronegativities[21] (right scale) of the alkali metals. For further computational details, see reference 20.

The ionic nature of the C-M bond is supported by the fact that most polar organometallics react by ionic mechanisms.[22-28] However, this does not

mean that RM reagent differing only in the metal (M = Li, Na, K, Rb, Cs) always give the same product. On the contrary, the regiospecificity is often critically dependent on the size/charge ratio (Table 2.1), and will therefore frequently yield different products with different gegenions.[27,29,30] This, of course, is a combined effect of gegenion, carbanion and solvent resulting in different ionpairing and aggregation effects.

Table 2.1. Table of relations of charge and surface of the gegenions Li^+ to Cs^+.

Ion	Radius[31] /pm	surface/ 10^{-20} m^3	consecutive surface ratio	surface ratio relative to Li^+
Li^+	76	7.26	1.00	1.00
Na^+	102	13.1	1.80	1.80
K^+	138	23.9	1.83	3.30
Rb^+	152	29.0	1.21	4.00
Cs^+	167	35.0	1.21	4.83

It is well established that the increasing ion surface, going from Li to Cs, leads to an increasing fraction of CIPs, mainly due to the greater polarisability and less solvation of the larger gegenions. Generally, the tendency for aggregation decreases going from Li^+ to Cs^+.

X-ray structures of polar organometallic compounds show that coordination numbers to Li^+ ranges from two through seven[25] thus these compounds do not seek to fulfil the "octet rule".[19]

2.3 Ionpairing

The recognition of ionpairing effects in carbanion chemistry followed upon the work of Grunwald,[32] Winstein and coworkers,[33] and Fuoss and coworkers.[33-35] They made the terms contact, tight or intimate ionpair and solvent separated or loose ionpair household names in the chemical community. Later, Marcus[36] introduced another useful term, the solvent-shared ionpair (Figure 2.4).

In contact ionpairs (CIP), the anion and cation are directly in contact with each other and are surrounded by a common solvation shell. In solvent-shared ionpairs (solvent bridged ionpairs[37] = SBIP), the ions are bridged by one or more solvent molecules. In the solvent-separated ionpairs (SSIP) the solvation shells of the ions are in contact with each other.

Figure 2.4. Ionpair equilibrium.

The first direct observation of such postulated[33,38] ion pairs was made by Hogen-Esch and Smid by means of UV-vis spectroscopy.[39-41] They soon established that the equilibrium in Figure 2.4 was dependent on temperature, gegenion, solvent and pressure. The relationship studied, mainly dealt with the CIP/SSIP equilibrium. The fraction CIPs increases with larger gegenions. The fraction of SSIPs increases with the polarity of the solvents, upon lowering the temperature and with increasing pressure. These early investigations were carried out with delocalised carbanions *e.g.* fluorenides. The reactivity increases in the order: CIP < SBIP < SSIP < solvated free ions.

Since 1966, several other techniques for ionpairing studies, such as NMR[42] spectroscopy and EPR (Electron Paramagnetic Resonance) spectroscopy have emerged.[43] An interesting note is that the temperature range over which a given type of ionpair is observed to dominate, may vary with the technique used.[43]

2.4 Aggregation

Aggregation is another complicating feature of studies of alkali metallation reactions. The reactivity of the organo alkali metal reagent is dependent on the aggregation. The aggregation plays an important role in stereoselective synthesis. The degree of aggregation also depend critically on the solvation and the type of cations. The majority of known aggregates can be built from a few simple structure patterns (Figure 2.5). It is striking from Figure 2.5 how large a role entropy plays in the equilibrium between different aggregation states.

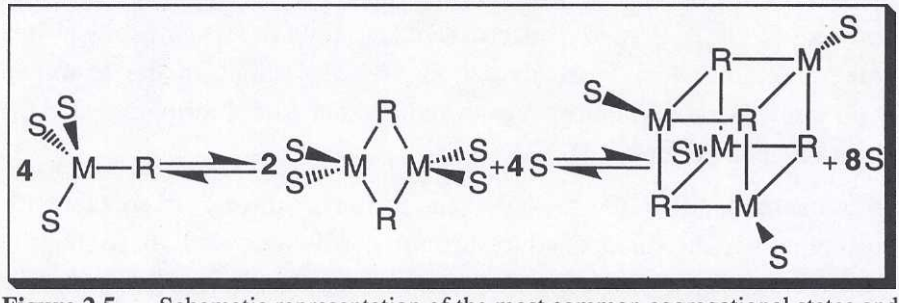

Figure 2.5. Schematic representation of the most common aggregational states and their equilibrium.

One of the most striking effects of aggregation is the solubility of n-BuLi in hydrocarbons. n-BuLi is a hexamer in hexane. This aggregate has a hydrophobic shell, enclosing the polar parts, similar to the structure of a

micelle. This has the effect that, besides its high solubility in hydrocarbons, $(n\text{-BuLi})_6$ also has a low boiling point and a low melting point compared with *e.g.* n-BuCs, which does not aggregate.[19,44] These properties led chemists erroneously to believe that the C-Li bond was covalent.

Usually the reactivity increases in the order from large aggregates to small aggregates, *e.g.* hexamer < tetramer < dimer < monomer. This has been explained in terms of dipole-dipole interaction and steric effects. Aggregation is mainly studied by NMR spectroscopy, colligative methods and X-ray diffraction.

2.5 Solvent effects

The discussion of solvent effects is mainly focused on the solvation of the cation, since the solvents used in alkali metallation reactions generally have poor solvating ability for carbanions. The carbanion may be viewed as a complexing agent that competes with the solvent molecules or other ligands for the solvation of the cation. The most commonly used solvents for lithiation reactions are tetrahydrofuran (THF), diethyl ether (DEE) and hexane. Other ethers such as dimethoxyethane (DME) and hydrocarbons, such as cyclohexane or benzene are occasionally used.[45] There are many examples where different products are obtained with different solvents.[46] Generally, more polar solvents facilitate alkali metallation reactions, due to increasing solvating ability of either the IS (solubillity), the TS or the end product. Unfortunately, they are often also more readily attacked by the alkali metal reagents (see 2.5.2).

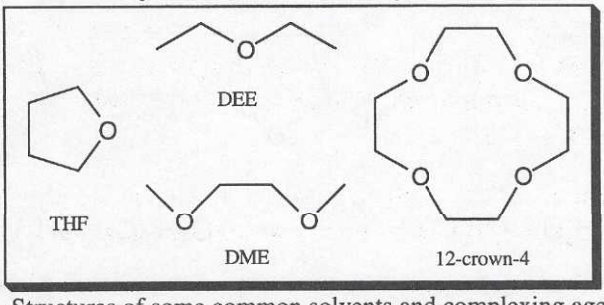

Figure 2.6. Structures of some common solvents and complexing agents in alkali metallation reactions.

DME is an interesting solvent since it is bidentate and well suited for ligation of lithium ions, unfortunately it is also more reactive than THF.

2.5.1 Complexing agents

Complexing agents, *i.e.* specific cation ligands that are present in such low concentrations that they cannot be considered as solvent molecules, are used to manipulate the effects of ionpairing and aggregation. Some of the most commonly used complexing agents are 12-crown-4, which is used mainly to create SSIP since it hides the cation in its crown, and tetra-methyl-ethylenediamine (TMEDA) which is used to break up larger aggregates into smaller ones in order to increase the reactivity. The idea is to have a molecule with higher specificity for the cation than that of the solvent molecules - but not necessarily than that of the carbanion - in order for it to be able to compete with the abundant solvent molecules.

2.5.2 Stability of alkali metal reagents in solvents

The major disadvantage in the use of more polar solvents such as ethers, is that they are readily cleaved by some alkali organometallic reagents. Thus reactions conducted in such solvents can be considered as competition reactions between the solvent and the substrate for the metallating reagent. The products in such competing reactions are often organometallic compounds as well (Figure 2.7), they therefore increases the overall complexity, *e.g.* by forming mixed aggregates and by being involved in further reactions.[46,47]

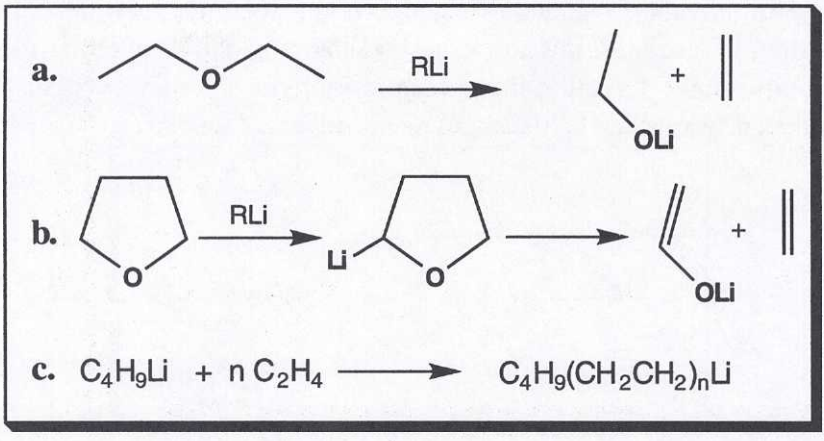

Figure 2.7. The cleavage of DEE (a) and THF (b) by RLi. Reaction (c) show the insertion of ethene created in reactions (a) and (b) (assuming a closed system). This reaction forms higher homologues of *e.g.* n-butyllithium.

Table 2.2 shows kinetic data concerning the stability of n-BuLi in often used solvents.

Table 2.2. Kinetic data on the stability of n-BuLi in common solvents.[46]

Solvent	Temperature/°C	t(1/2)
DEE	5	6 d
DEE	35	31 h
Di-isopropyl ether	25	18 d
Diglyme[a]	25	10 min
THF	0	23.5 h
THF	-30	5 d

[a] Diglyme = 2-methoxyethyl ether, $(CH_3OCH_2CH_2)_2O$

Even in inert solvents such as hydrocarbons there are competing reactions that consume the reagent, *e.g.* n-BuLi in hexane is thermally converted to 1-butene and lithiumhydride (Figure 2.8a). There are several other common sources of impurities in alkali metallation reactions. Figure 2.8 b-c show some common reactions of n-BuLi. Furthermore, it has been shown that alkali metal salts (MX), such as LiI, can influence the path and rate of alkali metallation reactions.[48]

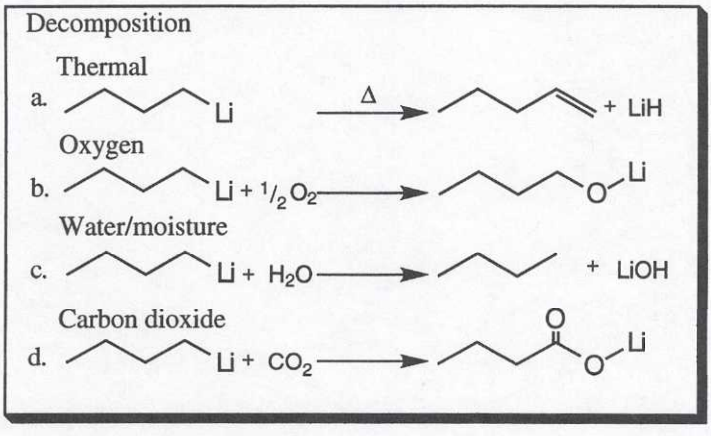

Figure 2.8. Some reactions of n-butyllithium

2.6 Structure and stability of carbanions

The effect of the carbanion is mainly related to what extent the negative charge can be delocalised and to steric requirements. The nature of the carbanion can be dealt with by classical organic chemistry terminology by looking at such effects as hybridisation, conjugation, aromaticity, dipole-stabilising, polarisability, negative hyperconjugation, and inductive effect.[49]

The stabilities of the carbanions are measured by the pKa values of the corresponding carbon acids. However, there are several problems to consider. To obtain the intrinsic effect of the carbanion, the effect of gegenion, solvation, ionpairing etc. should be subtracted.
In this context, we are dealing with compounds giving localised carbanions *e.g.* methane ($pK_a \approx 48$) to delocalised carbanions *e.g.* fluorene ($pK_a \approx 23$).

Table 2.3. Table of pK_a's for selected compounds.[50,51]

Compound	pK_a	Compound	pK_a
Cyclopentadiene	16	Toluene	41
Indene	20	Benzene	43
Fluorene	23	Methane	48
Triphenylmethane	31.5	Ethane	50
DMSO (CH_3SOCH_3)	33	Cyclohexane	51

3 [1.1]Ferrocenophanes - background

This section briefly describes the background of ferrocenophane (FCP) chemistry in general and [1.1]ferrocenophane chemistry in particular.

3.1 History and significance

The story of [1.1]ferrocenophanes begins in the early 1950's with the synthesis of ferrocene[52,53] and the understanding of its unusual properties.[54,55] The discovery of this sandwich complex, initiated a wide spread research activity to explore this field. One branch that developed was ferrocenophane chemistry. Ferrocenophanes are compounds that contains one or more ferrocene units connected with one or more bridges of carbon atoms (Figure 3.1).

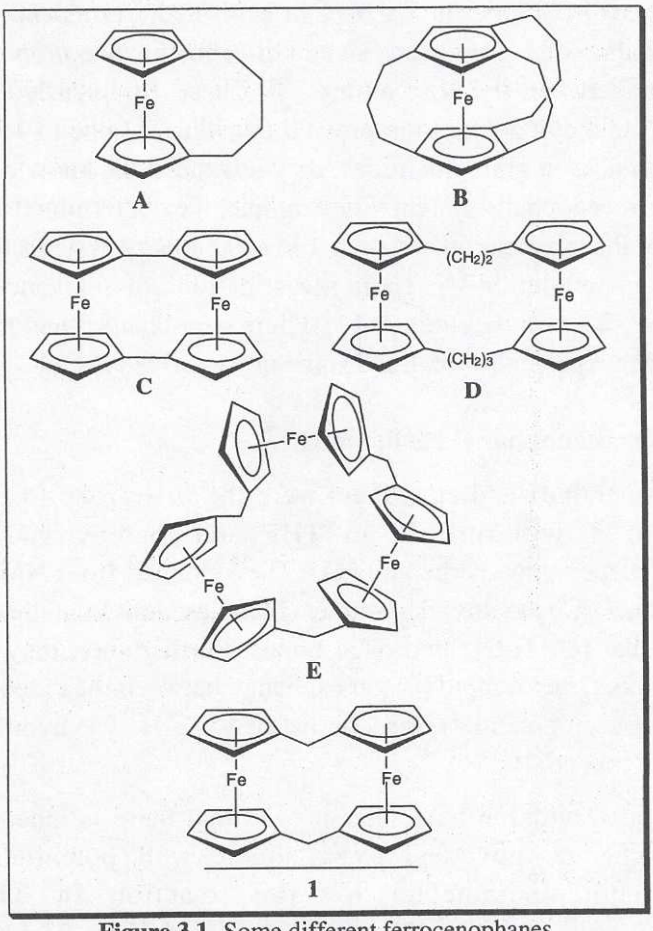

Figure 3.1. Some different ferrocenophanes.

The naming of these compounds stems from a nomenclature published by Smith in 1964,[56] and is applicable to all bridged aromatic species. The basic notations are: [m]ferrocenophanes for monoferrocene FCPs, *e.g.* [4]ferrocenophane (A) and [4][3][3]ferrocenophane (B), [m.n]ferrocenophanes for diferrocene FCPs, *e.g.* [0.0]ferrocenophane (C) and [3.2]ferrocenophane (D), [m.n.o]ferrocenophanes for triferrocene FCPs *e.g.* [1.1.1]ferrocenophane (E) etc.

The [m]ferrocenophanes attracted most of the attention in the early days and it was not until 1966 that 1,12-dimethyl[1.1]ferrocenophane (DMFCP) (**3**) was synthesised by Watts,[57] as the fourth [m.n]ferrocenophane. The year after, the parent compound [1.1]ferrocenophane (**1**) also was synthesised by Watts, but in very poor yield.[7]

In the decade that followed, several interesting aspects of the chemistry of **1** were discovered. Dissolution of **1** in acid media produced hydrogen gas.[58] Oxidation of **1** formed mono- and di-cations with a proposed direct interaction between the iron atoms.[59,60] These findings led Mueller-Westerhoff and coworkers to improve the synthetic route to **1** in 1981.[11] With **1** available in gram quantities, they advanced the knowledge about the [1.1]ferrocenophane system. For example, they determined the crystal structure of the monocation and used **1** in solar energy systems to catalyse hydrogen gas evolution.[1,61] Their investigations of relevance for this thesis, were those on deprotonated [1.1]ferrocenophanes[2] and that on the conformational properties of **1** and some of its derivatives.[62]

3.2 [1.1]Ferrocenophanyl carbanions

Mueller-Westerhoff and coworkers were the first group to report the reaction of **1** with n-BuLi in THF and thereby yielding the 1-[1.1]ferrocenophanyl carbanion (**2**).[2] They claimed from NMR studies of **2** and some of its methyl derivatives, that these ions contained the first intramolecular $[C\cdots H\text{-}C]^-$ hydrogen bonds. Furthermore, they observed that there was either a rapid proton exchange between the carbon bridges of **2** (double well potential) or a symmetrical $[C\cdots H\cdots C]^-$ hydrogen bond (single well potential).

Ahlberg and Davidsson have later proved that there is indeed a rapid proton exchange, governed by a double well potential.[3-5] The thermodynamic parameters for this reaction in THF are; $\Delta G^{\ddagger}$= 42 kJ mol^{-1} (-24 °C), $\Delta H^{\ddagger}$= 19 kJ mol^{-1} and $\Delta S^{\ddagger}$= -93 J K^{-1} mol^{-1}.

The large negative entropy of activation implies an increased order in the transition state, *e.g.* an extra solvent molecules is bonded in the transition state.

These investigations led to the discovery that the [1.1]ferrocenophanyl alkali metals are useful models for the investigation of alkali metallation reactions. Some introductive studies have been performed by Öjvind Davidsson and are presented in his thesis from 1990.[5]

3.3 The conformational saga of [1.1]ferrocenophanes

Mechanical models show that [1.1]ferrocenophanes may adopt two main conformations, a *syn*-conformation and an *anti*-conformation (Figure 3.2). Substituents on the carbon bridge are defined as being either *exo* or *endo* relative to the iron atoms (Figure 3.2).

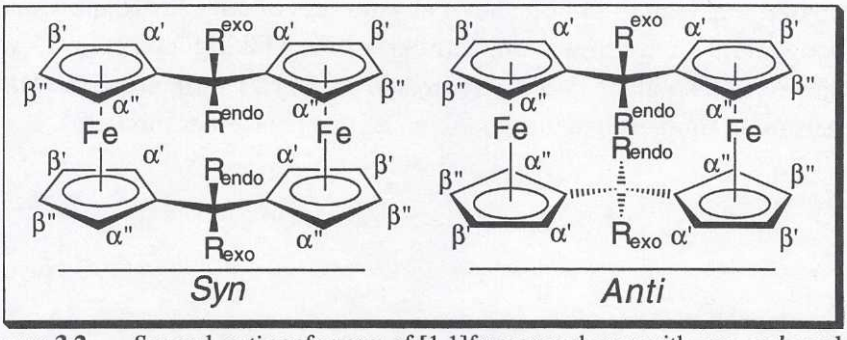

Figure 3.2. *Syn* and *anti* conformers of [1.1]ferrocenophanes with *exo*, *endo* and ring positions marked.

The existence of an *anti*-conformation of the [1.1]ferrocenophanes has been debated ever since the first conformational investigations made by Watts in 1966.[57] Watts suggested, tentatively, that the newly prepared 1,12-dimethyl-[1.1]ferrocenophane (DMFCP) should have a twisted *anti*-conformation due to "non bonded interaction between methine protons" as well as between the α' protons in the completely planar (C_{2v} type) *syn*-conformer **1**. However, later X-ray studies of crystals obtained from DMFCP, proved the presence of a twisted *syn*-conformer,[8,9] *i.e.* *exo,exo,syn*-1,12-dimethyl-[1.1]ferrocenophane.

Another conformational feature was revealed with the parent compound [1.1]ferrocenophane (**1**). Right from the beginning, Watts suggested that **1** has an unusual flexibility,[7] *i.e.* undergoes a fast complex internal conformational inter conversion. This process was suggested to explain the simple NMR spectrum of **1**, which shows only three signals. Already

in 1967, Watts concluded with the aid of Dreiding models that the "eclipsed" conformer (*syn*) was much more flexible than the "staggered" conformer (*anti*), and that the *syn*-conformer could easily undergo a degenerate rearrangement. He also stated that "Models also indicate that inter conversion of the eclipsed and staggered configurations can occur only at the expense of gross deformation of preferred bond angles and distances and is therefore considered improbable".[7] As a result, Watts and subsequent researchers[2,10,11,61,62] believed that the preferred (and only) type of conformer of [1.1]ferrocenophanes is a twisted *syn*-structure, with the possibility of a "*syn-syn*"[11] exchange reaction.

In 1969, Watts and coworkers presented evidence for a second isomer of DMFCP, which they tentatively assigned the structure *exo,endo,syn*-1,12-dimethyl-[1.1]ferrocenophane. Mueller-Westerhoff and coworkers prepared this isomer in large amounts and reported its NMR spectrum.[11] A degenerate rearrangement, similar to that taking place in **1**, was assumed to take place in the *exo,exo,syn*-isomer as well, since the NMR spectrum is simpler than the symmetry of this conformer implies.

4 Experimental

In the investigations of the [1.1]ferrocenophanyl alkali metals and the [1.1]ferrocenophanes, we have applied several experimental methods, which are described below.

4.1 Methods

4.1.1 Solution NMR spectroscopy

Multinuclear 1D NMR spectroscopy has mainly been used for structural elucidation and determination of the purity of both compounds and solvents. It has been used to measure slow intermolecular lithiation reactions.

1 D Dynamic NMR spectroscopy (1D DNMR) is extremely useful in the study of exchange processes. Rate constants and activation parameters have been determined for degenerate processes.[63]

2D NMR spectroscopy, especially ^{1}H-^{1}H, Nuclear Overhouse Effect SpectroscopY (NOESY) have been used for structure elucidation. NOESY give information about atoms that are close in space and about exchange processes. In our investigations, one of the limiting factors in the use of especially 2D techniques has been the high symmetry of our compounds either due to their structure or because of dynamic processes.

All solution NMR experiments have been carried out on a Varian XL-400 spectrometer (^{1}H observation frequency 400 MHz) and a Varian Unity 500 spectrometer (^{1}H observation frequency 500 MHz) equipped with three channels. The low temperature control system consists of a "long hold VT - liquid nitrogen Dewar with a heat exchanger", attached to a mixer for mixing "cold" and "warm" nitrogen. The gas regulation system for the nitrogen flows was designed and produced at this department (see Figure 4.1).[64]

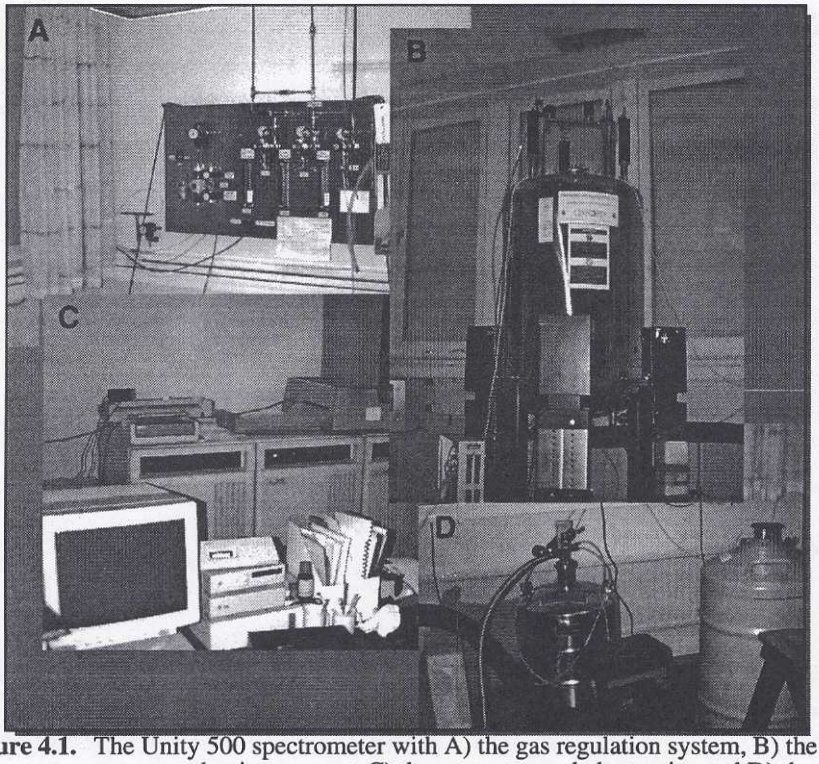

Figure 4.1. The Unity 500 spectrometer with A) the gas regulation system, B) the super conducting magnet, C) the computer and electronics and D) the liquid nitrogen Dewar.

4.1.2 NMR- and Dynamic NMR-spectroscopy - simulations

In Dynamic NMR spectroscopy, information about the rate constant of the process that is monitored is derived from the bandshapes and shift difference of the signals involved. In the case of a first order spectrum with singlets, a manual estimation from simple equations may suffice.[5] In more complicated cases, where the signals involved are not part of a first order spectrum or if they are multiplets, complete bandshape analysis by simulations becomes necessary to obtain accurate rate constants.[63] For this purpose programs like DNMR5[65] and the program developed by Fraenkel and coworkers (se reference 66 for details of the method behind the program) have been used.

In order to perform simulations, the spectral data from a slow exchange spectrum, *i.e.* chemical shifts and coupling constants are used as input data together with the T_2 (transverse relaxation time) and the proposed mechanism. Rate constants are guessed and the program calculates the corresponding spectra. These spectra are then visually compared with the

experimentally recorded ones, and this process is then repeated until the best fit is achieved. Normally DNMR experiments use a variation of temperature to vary the rate. This makes it possible to determine activation parameters; $\Delta G^{\ddagger}$, $\Delta H^{\ddagger}$ and $\Delta S^{\ddagger}$.
One type of input parameters for DNMR5 are the coupling constants, which can be hard to estimate from complex multiplets. Therefore we used normal 1D NMR simulations[67] to estimate the coupling constants in complicated cases.

4.1.3 Solid-state NMR spectroscopy

Solid state NMR has been used to study conformers in the solid state. A transfer to the solid state dramatically slows down dynamic processes.

Solid state NMR experiments were performed on a Varian VXR-300 (^{13}C observation frequency 75.4 MHz) equipped with a Varian variable temperature CPMAS (Cross Polarisation Magic Angle Spinning) probe.[68]

4.1.4 X-ray crystallography

Detailed structural information of solid state structures was obtained by X-ray diffraction.

The diffractometric studies were made with a Rigaku AFC6R diffractometer, the structures solved with direct methods (MITHRIL[69]) and all calculations performed with the TEXSAN[70] program package.[71]

4.1.5 UV-vis spectroscopy

UV-vis spectroscopy have mainly been used to investigate the temperature dependence of the CIP/SSIP equilibrium of alkali metal salts of [1.1]ferrocenophanes in different solvents and with complexing agents. The technique has also been used to study the kinetics of lithiation of [1.1]ferrocenophane.

The equipment used was a Cary 04 spectrophotometer, an Oxford variable temperature liquid nitrogen cryostat model DN1704 equipped with an ITC-4 temperature controller. The temperature close to the sample was monitored with a S25421 Thermolyzer (Systemteknik, Lidingö, Sweden) equipped with a Pt100:1/10 DIN temperature sensor.

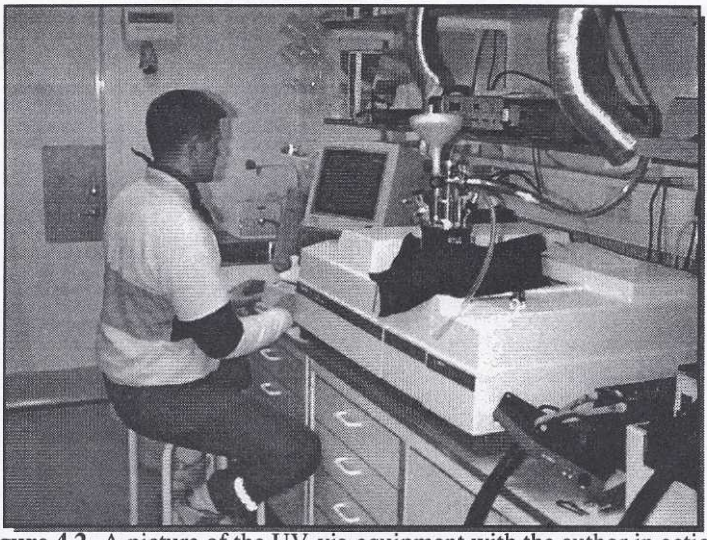

Figure 4.2. A picture of the UV-vis-equipment with the author in action.

It is possible to operate the cryostat in the temperature range from 77K (liquid nitrogen) to 500 K. The cuvettes were from Helma (No. 220-QS, 1 mm and 10 mm) onto which the top of a Wilmad/omnifit system, 507-OF NMR tube is welded. The Wilmad/omnifit valve assembly (OFV) was used to seal the cuvette (Figure 4.3)

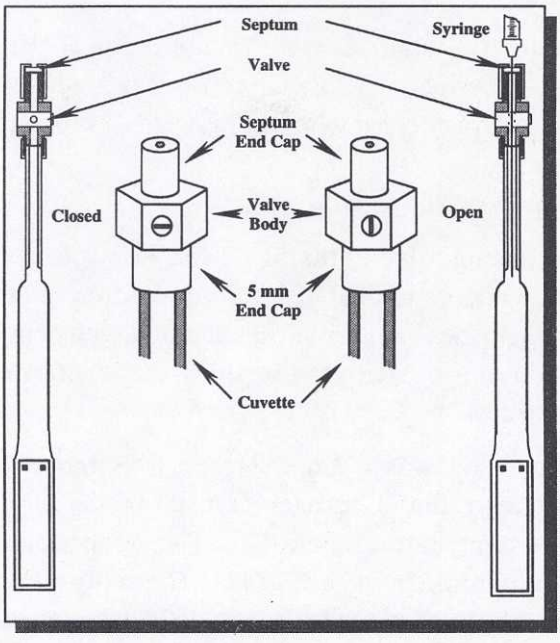

Figure 4.3. The cuvette with the Wilmad/omnifit system.

4.1.6 Computer aided visualisation

Computer aided visualisation was used as an efficient tool to comprehend structural information such as bond distances, bond angles etc. The possibility of rotating *e.g.* a X-ray structure on the screen is a major advance for chemical comprehension. A further development in visualisation of the conformational behaviour of [1.1]ferrocenophanes has been to make a film of the pseudorotation of [1.1]ferrocenophane. This film is published on the Word Wide Web[72,73]
URL: http://www.che.chalmers.se/inst/oc.gu/people/jml-home/pseudo-fcp-movie.html.

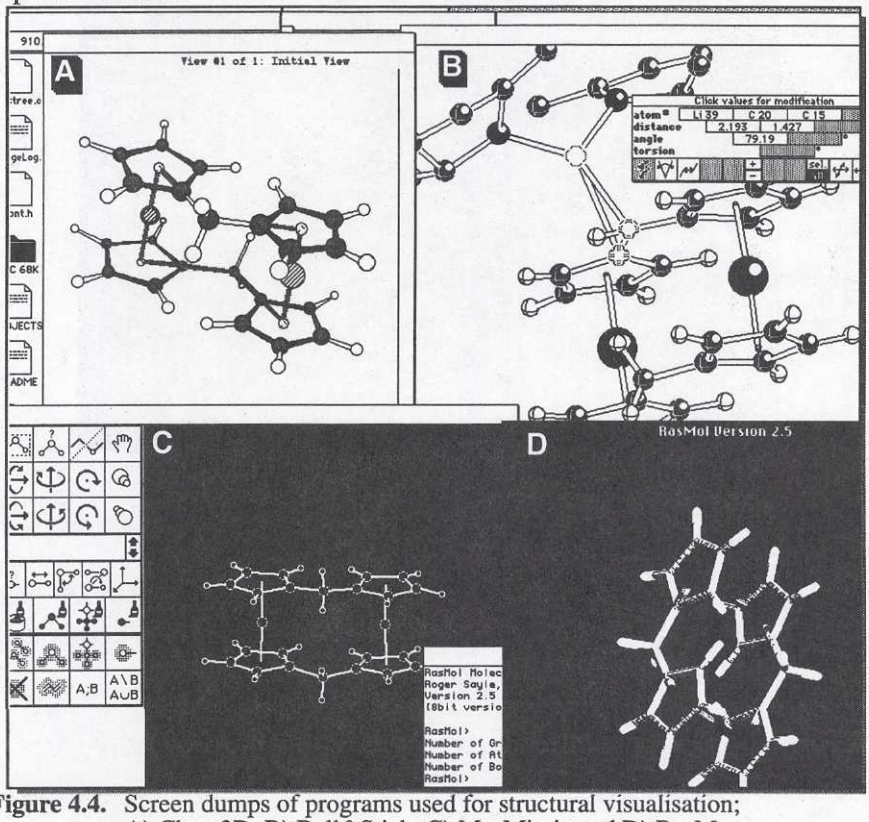

Figure 4.4. Screen dumps of programs used for structural visualisation; A) Chem3D, B) Ball&Stick, C) MacMimic and D) RasMac.

Programs used for these purpose were Chem3D,[74] Ball&Stick,[75] MacMimic[76] and RasMac.[77]

4.1.7 Mechanical models

A very important part of the process of understanding the conformational properties of [1.1]ferrocenophanes was the utilisation and development of mechanical models.[78] Models were built with ball bearings and steel springs that allowed the model to show some of the flexibility that we gradually found from experimental results. Hours of contemplation with these models in hand, have given insights and ideas otherwise very hard to reach.

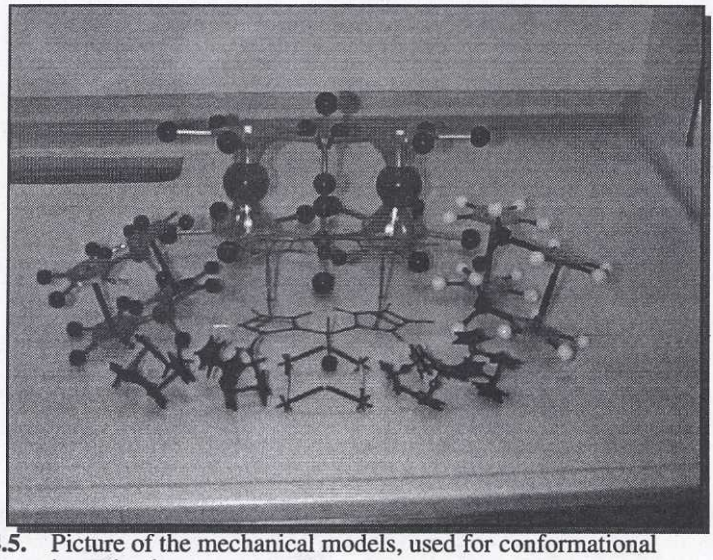

Figure 4.5. Picture of the mechanical models, used for conformational investigations.

4.1.8 Isotopic labelling

Compounds labelled with ^{13}C or ^{2}H were produced in order to facilitate NMR spectroscopic investigations. To some degree, these compounds were used to study isotop effects on rate constants.

4.2 Chemical preparations and Experimental procedures

4.2.1 General

All nondeuterated solvents were distilled in a nitrogen atmosphere from sodium/benzophenone prior to use unless otherwise stated. The deuterated solvents were stored over Deperox® (Fluka AG), degassed and distilled on a vacuum line.

All handling of chemicals was in an inert atmosphere (nitrogen or argon), unless otherwise stated. The Nitrogen gas quality used was AGA-Plus (less than 5 ppm O_2 and H_2O) and the Argon quality was AGA-Plus (less than 5 ppm O_2 and H_2O).

All references to a vacuum line concerns the system consisting of a Trivac S/D 1.6 B and a Turbovac® 50 from Leybold AG, unless otherwise stated. Pressures obtained with this vacuum line were typically $1\text{-}2\text{x}10^{-6}$ torr.

All references to a glove box concern the Mecaplex GB-80, unless otherwise stated. The glovebox is equipped with a gas-purification system which removes water and oxygen from the nitrogen atmosphere of the box. The water content in the glovebox atmosphere was measured with a Shaw hygrometer (model SHA-TR). Typically, the content is 1-2 ppm at atmospheric pressure.

Only gas-tight syringes (Unimetrics and Hamilton) were used.

The procedure for the preparation of carbanions of **1** and **3** for most NMR experiments except the "catalysis experiment" (*vide infra*), is described in reference.[5]

4.2.2 Synthesis of [1,12-$^{13}C_2$]-[1.1]ferrocenophane (^{13}C-1)

The synthesis of **^{13}C-1** is analogous to that of the unlabelled compound, *i.e.* **1**.[11] The synthetic route to **^{13}C-1** (Figure 4.6) involves preparation of the following compounds: a $FeCl_2$-THF complex, 6-(dimethylamino)-[6-^{13}C]-fulvene, 1,1'-dilithioferrocene and 1,1'-bis(6-[6-^{13}C]-fulvenyl)-ferrocene.

The ^{13}C source was dimethyl[^{13}C]formamide, labelled at the carbonyl carbon (isotope purity 99 atom%, chemical purity >98%), purchased from Cambridge Isotope Laboratories. The ^{13}C content was measured only in the target molecule.

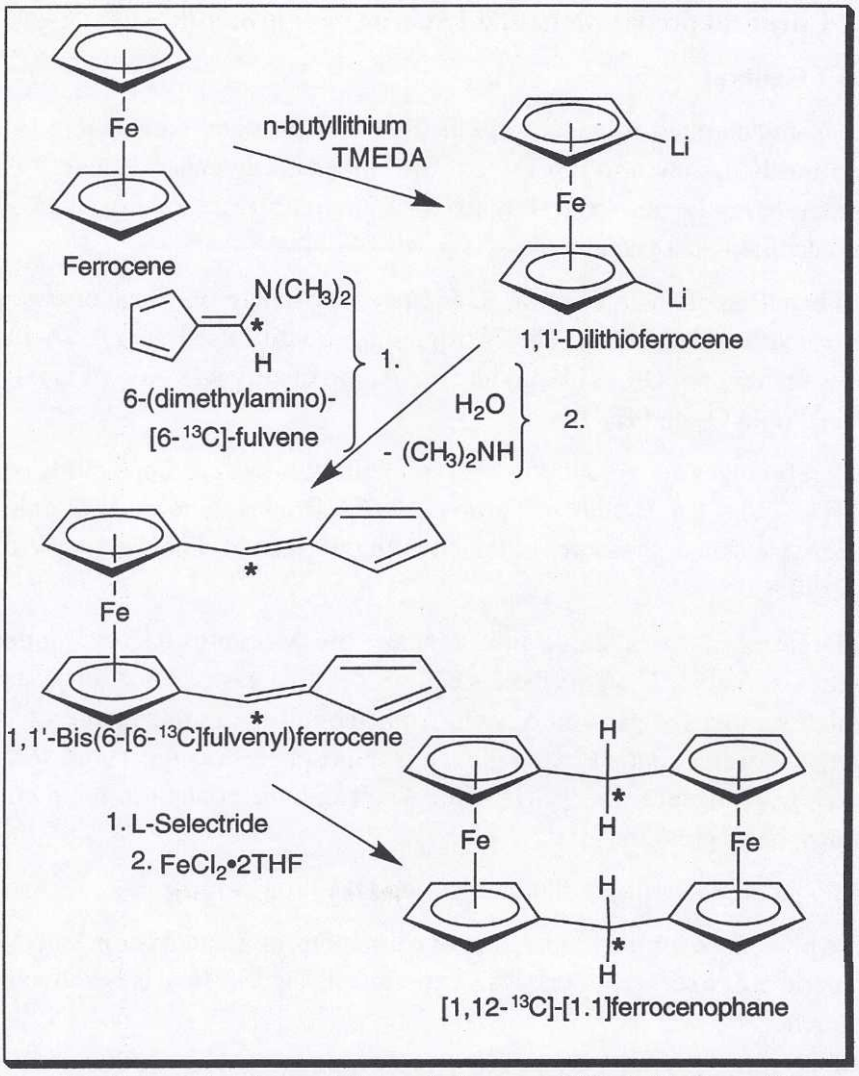

Figure 4.6. General description of the synthetic route of **^{13}C-1**. * indicates ^{13}C.

Preparation of $FeCl_2$-THF complex. This complex was prepared according to the literature,[79] (Figure 4.7) in quantities up to 25 grams each time. The product was stored in the freezer in glass flasks put in plastic bags filled with nitrogen.

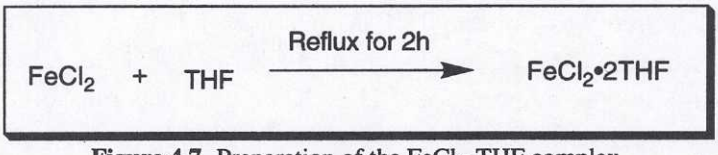

Figure 4.7. Preparation of the $FeCl_2$-THF complex.

Preparation of 6-(dimethylamino)-[6-^{13}C]fulvene. This compound was made from 1.0 g (0.0137 mol) N,N'-dimethyl[^{13}C]formamide analogously to the unlabelled compound (Figure 4.8).[80] The product was stored in the freezer and used the following day. The crude yield was 1.172 g (71%). (literature value for the unlabelled compound: 69-76%).

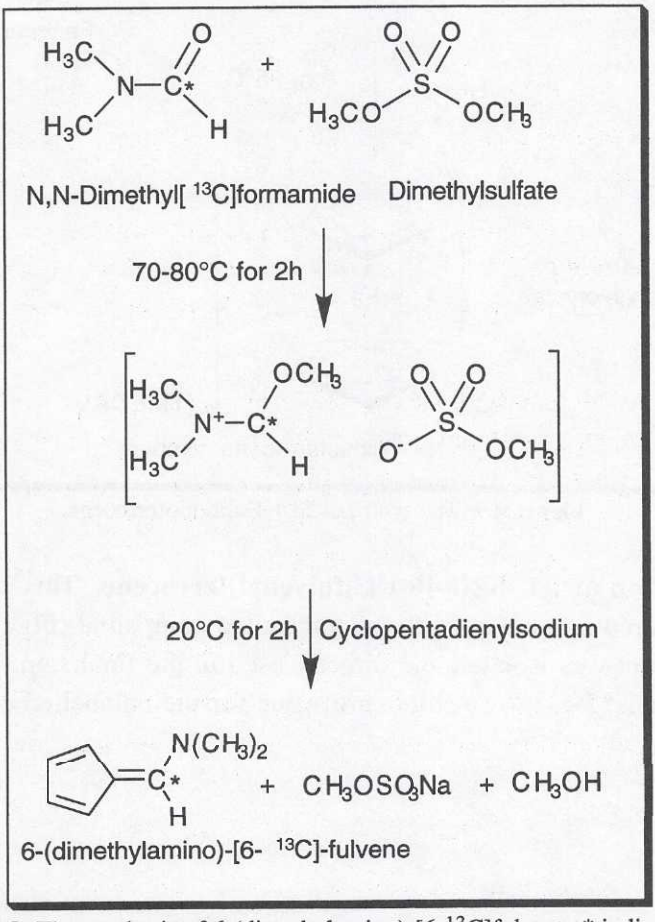

Figure 4.8. The synthesis of 6-(dimethylamino)-[6-^{13}C]fulvene. * indicates ^{13}C.

Preparation of 1,1'-dilithioferrocene. This compound was prepared according to the literature (Figure 4.9).[81] The crystals of 1,1'-dilithioferrocene[82] were washed and suspended in hexane for direct use in the next step.

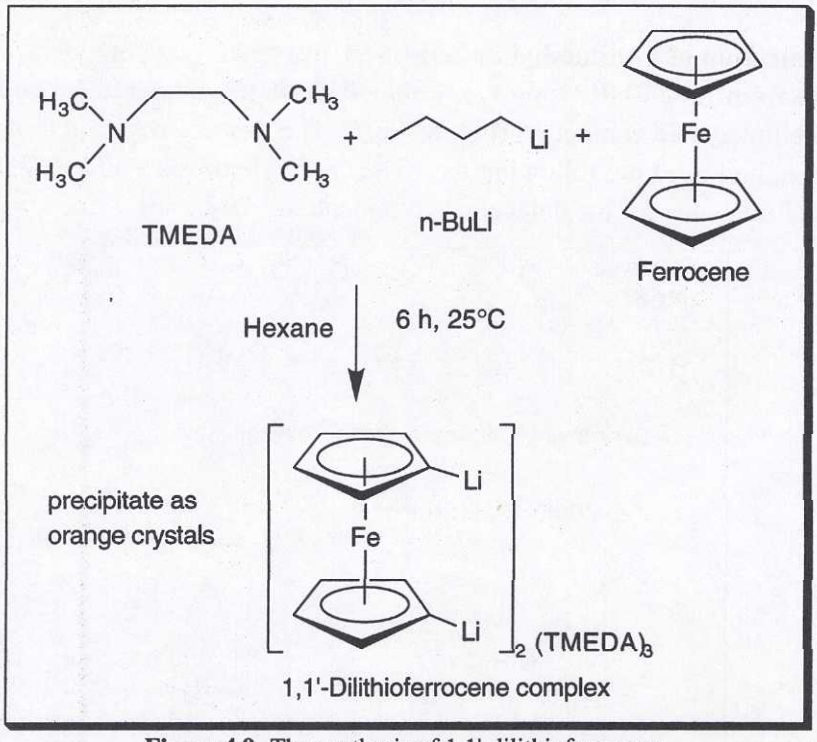

Figure 4.9. The synthesis of 1,1'-dilithioferrocene.

Preparation of 1,1'-bis(6-[6-^{13}C]fulvenyl)ferrocene. This compound was prepared in analogy with the unlabelled compound (Figure 4.10).[11] The product was isolated and directly used in the final step. The crude yield was 1.57 g, (96%) (literature value for the unlabelled compound: 80-88%).

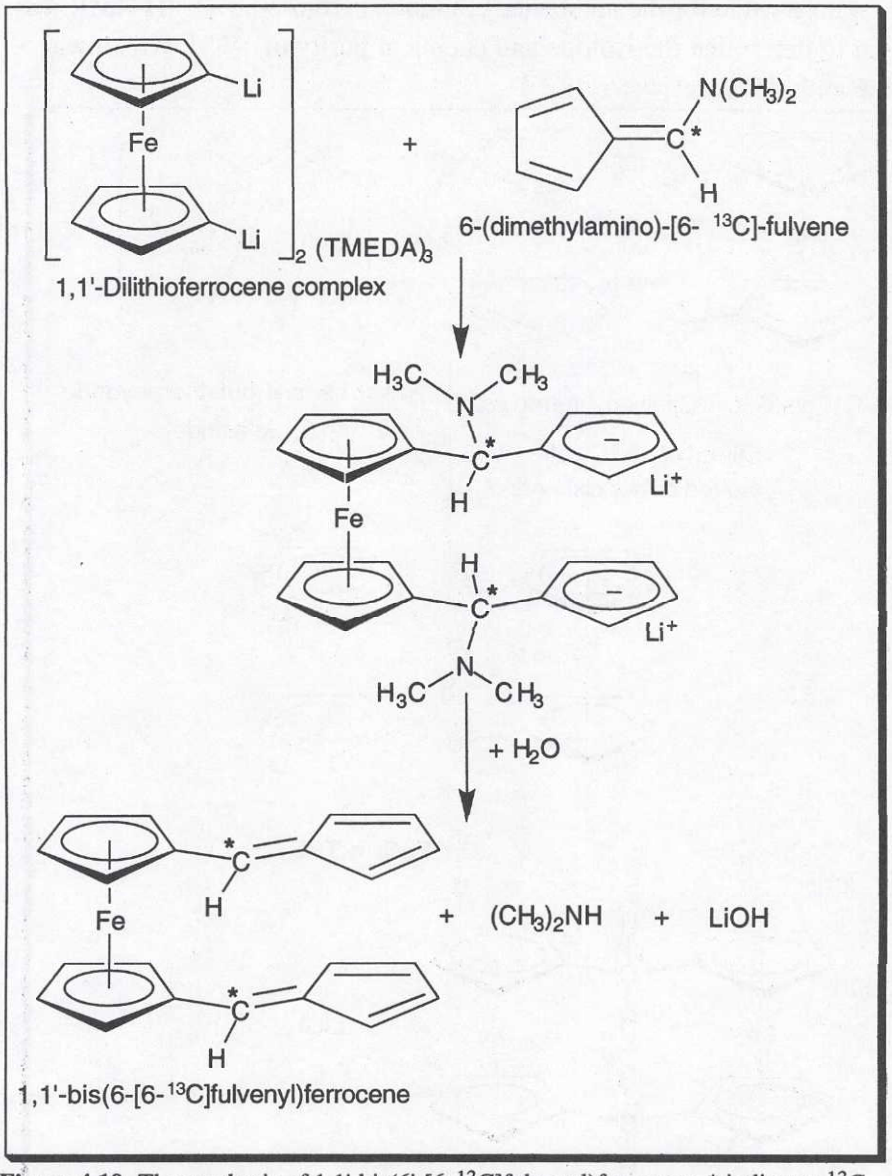

Figure 4.10. The synthesis of 1,1'-bis(6'-[6-^{13}C]fulvenyl)ferrocene. * indicates ^{13}C.

Preparation of [1,12-$^{13}C_2$]-[1.1]ferrocenophane (^{13}C-1). This compound was prepared in analogy with the unlabelled compound (Figure 4.11), using the "high dilution" method.[11] The product was isolated and directly transferred to the glovebox. The total yield relative to N,N'-dimethyl[^{13}C]formamide was 0.630 g, 1.6 mmol (23.4%)

(literature value for the unlabelled compound: 16.6-30.8%). ^{1}H NMR was used to determine the isotope and chemical purity of ^{13}C-1, which was > 98% and >99%, respectively.

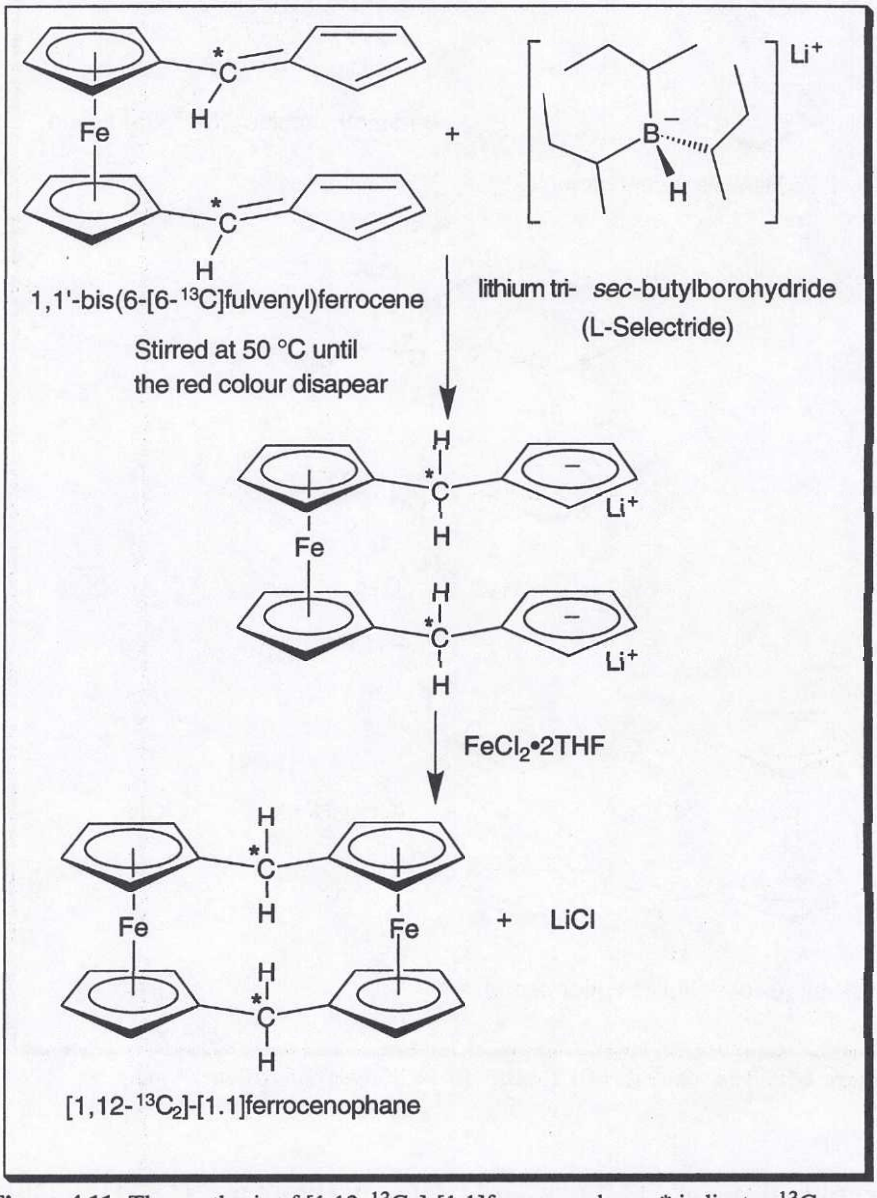

Figure 4.11. The synthesis of [1,12-$^{13}C_2$]-[1.1]ferrocenophane. * indicates ^{13}C.

4.2.3 Synthesis of 1,12-([23,24-$^{13}C_2$]-dimethyl)-[1.1]ferrocenophane (^{13}C-3)

The synthetic procedure for **^{13}C-3** (Figure 4.12) was similar to the synthesis of **^{13}C-1**. L-selectride was exchanged for methyllithium. In order to reach the target product 1,12-([23,24-$^{13}C_2$]-dimethyl)-[1.1]ferrocenophane, the ^{13}C-labelled carbon has to be introduced with [^{13}C]-methyllithium, prepared from [^{13}C]-methyl iodide (99 atom %, purity >98%). [^{13}C]-Methyl iodide was purchased from Euriso-top .

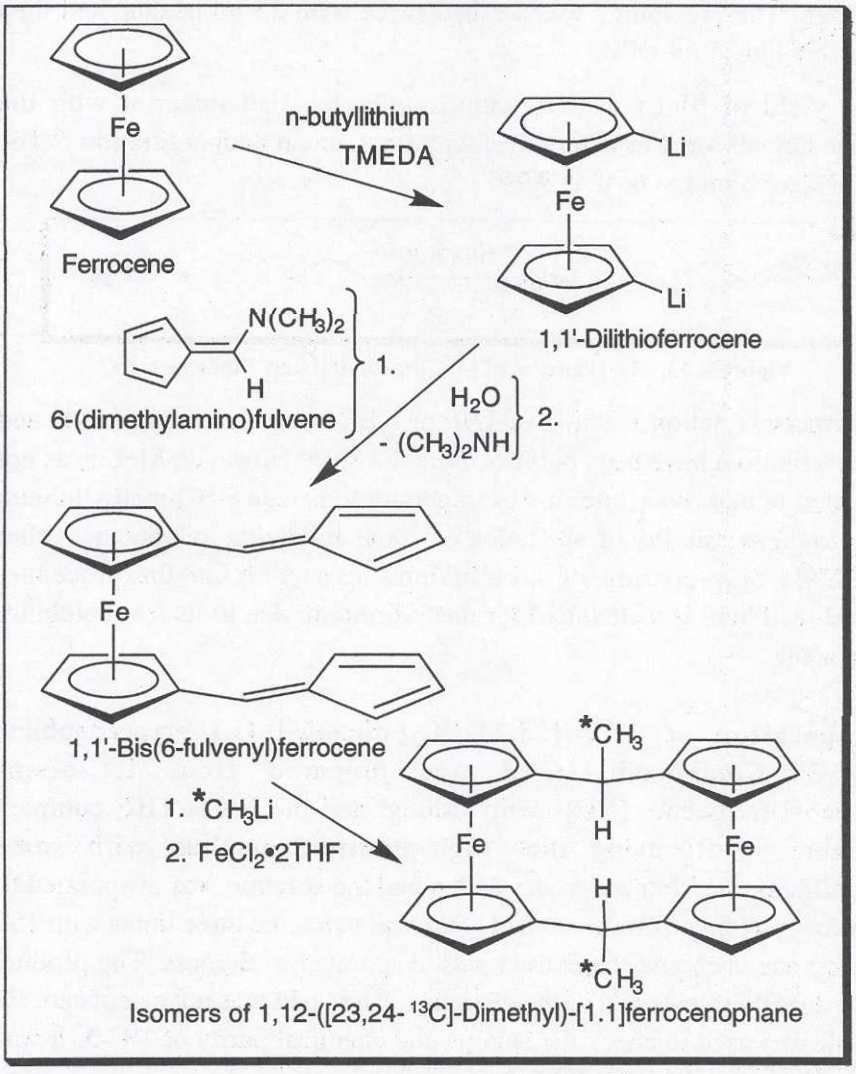

Figure 4.12. General description of the synthetic route of **^{13}C-3**. * indicates ^{13}C.

Preparation of [^{13}C]-methyllithium (Figure 4.13). A glass container equipped with two screw caps and a magnet was loaded with 25 ml n-BuLi (1.6 M in hexane), 40 mmol. The solution was cooled to -78°C in a CO_2(s)/ethanol bath and 2.15 ml (35 mmol) [^{13}C]-methyl iodide was added. The ethanol bath was slowly allowed to reach -30°C, when MeLi began to precipitate. The temperature was kept between -30 and -20°C for 2 hours, and the solution was then allowed to reach room temperature. The flask was centrifuged, and the supernatant was removed with a syringe. The precipitate was washed twice with 25 ml hexane and then dissolved in 25 ml DEE.

The yield of MeLi in preparations of unlabelled material with the procedure above, was determined with the Gilman double titration.[23] The yield were found to be over 95%.

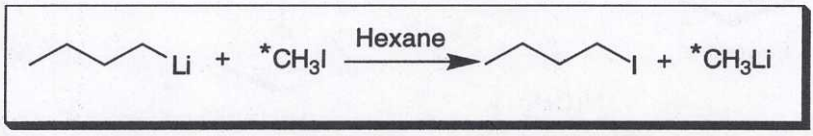

Figure 4.13. The synthesis of [^{13}C]-methyllithium * indicates ^{13}C.

The transalkylation reaction in THF or DEE between methyl iodide and n-butyllithium have been published previously.[83] However, MeLi was not isolated in that procedure. It was important to isolate [^{13}C]-methyllithium due to the possibility of alkylation reactions involving iodobutane. Other methods of preparing of alkyllithiums exist,[84,85] but the procedure developed here is well suited for methyllithium, due to its low solubility in hexane.

Preparation of 1,12-([23,24-$^{13}C_2$]-dimethyl)-[1.1]ferrocenophane (^{13}C-3). Compound **^{13}C-3** was prepared from 1,1'-bis(6-fulvenyl)ferrocene, [^{13}C]-methyllithium and the $FeCl_2$-THF complex (Figure 4.14), using the "high dilution" method with some modifications.[11] No water was added and the solution was evaporated to dryness yielding a crude product. This was extracted three times with 150 ml hexane each and the extract was evaporated to dryness. The product was directly transferred to the glovebox. The yield was not calculated. ^{1}H NMR was used to check the isotope and chemical purity of **^{13}C-3**. It was found to be > 98% and >99%, respectively.

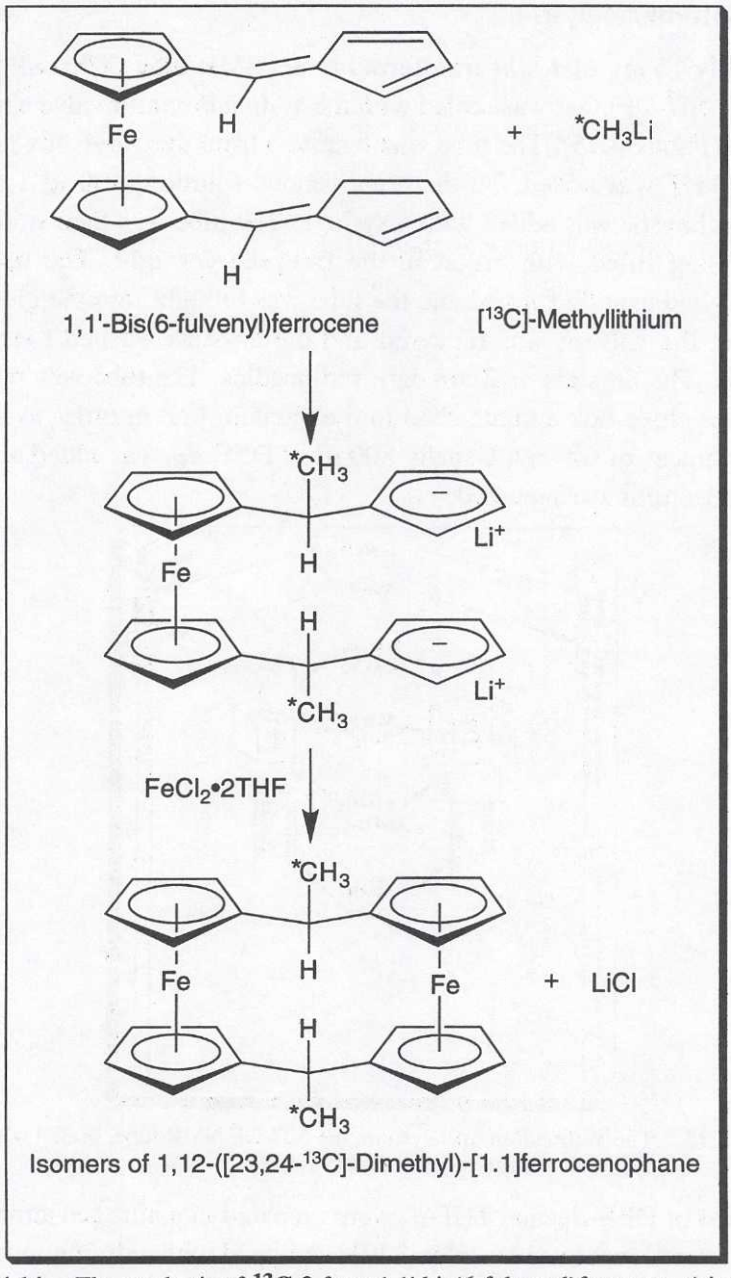

Figure 4.14. The synthesis of **^{13}C-3** from 1,1'-bis(6-fulvenyl)ferrocene. * indicates ^{13}C.

4.2.4 Solvent catalysis

Typically 15 mg of **1** was transferred to an NMR tube (Wilmad/omnifit system, 507-OF) that was sealed with the Wilmad/omnifit valve assembly (OFV) (Figure 4.15). The tube was removed from the glove box and 250 µl DMTHF was added. To the homogenous solution, 100 µl 1.6 M n-BuLi in hexane was added with a syringe. The tube was then stored in a plastic bag filled with argon in the freezer overnight. The next day crystals had usually formed and the tube was brought into the glovebox. Most of the solvent was removed and the crystals washed twice with heptane. The crystals of **2** are dark red needles. The tube was removed from the glove box and attached to the vacuum line in order to remove the last traces of solvent. Usually 800 µl of DEE-d_{10} was added and a ^{1}H NMR spectrum was recorded.

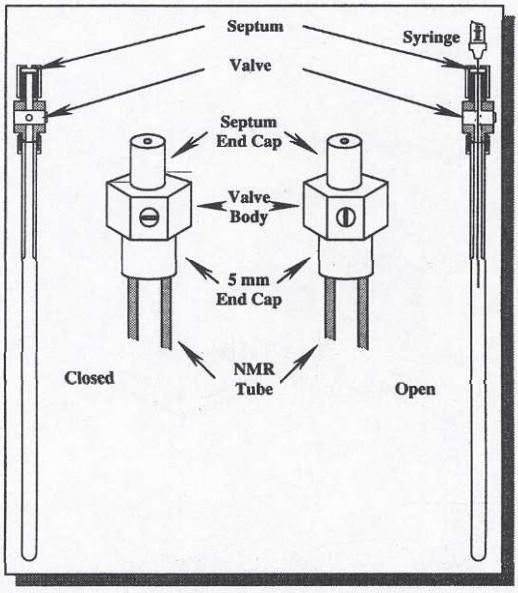

Figure 4.15. The Wilmad/omnifit system; the 507-OF NMR tube, sealed with the Wilmad/omnifit valve assembly (OFV).

Mixtures of DEE-d_{10} and THF-d_8 were prepared in a nitrogen atmosphere in a plastic glovebox (Mecaplex-2201, equipped with a drying tower with 4 Å molecular sieves). These mixtures were used for additions of small amounts of THF-d_8. All additions were made in the plastic glovebox using a 10 µl syringe. The tube was transferred to the NMR spectrometer and allowed to reach thermal equilibrium (27 °C), after which shimming was performed. A spectrum was recorded after each THF addition. Approximate rate constants were obtained from the signal due to the

proton on the carbanionic bridge carbon. These rate constants were used to guide the decision on the size of the next addition of THF. The final rate constants were determined from the band shapes using DNMR5. The same procedure was used for titration in other solvents, *e.g.* DMTHF and with other catalysts, *e.g.* DME.
Reproducibility was checked by preparing two different samples from two different crystallisations at the same time. The number of additions of THF and the amount in each addition was varied between the samples. The result can be seen in Figure 5.4.

4.2.5 Crystals for X-ray diffraction

[1.1]Ferrocenophanyllithium (2) in DMTHF. Crystals for X-ray diffraction were made in the same way as described for the catalysis experiment above. These crystals were handed over to M. Håkansson, who used his special low temperature handling techniques to isolate, select and mount crystals of **2**.[86]

[1.1]Ferrocenophane (1). Preparation of single crystals of **1** were made by M. Håkansson and the procedure is described in Paper V.

***exo,exo,syn*-1,12-Dimethyl[1.1]ferrocenophane (3a), *exo,exo,anti*-1,12-dimethyl[1.1]ferrocenophane (3b) and *exo,endo,syn*-1,12-dimethyl-[1.1]ferrocenophane (3c).** In the preparation of DMFCP[11] a mixture of isomers is obtained. This isomer mixture (9 g) was dissolved in 800 ml hexane by gentle warming. The temperature was lowered to approximately 4 °C, which resulted in the crystallisation of mainly **3a** after a few days.

The supernatant was decanted and evaporated to dryness, yielding a red powder. A portion of the red powder (100 mg) was dissolved in 5.0 ml of THF at ambient temperature. Crystallisation of **3c**, as intense red needles, was achieved by keeping the solution at 4°C for a few days.

The crystals of **3a** were immediately rinsed with 25 ml hexane and this solution was set aside at ambient temperature. Crystals of **3b** formed, as large red prisms, after a few weeks during which evaporation of most of the solvent took place.

Two types of crystals of **3a** were formed, orange-red cubes and orange-red needles. These crystals were separated by hand. The orange-red cubes

were found to be of the type reported before[9] and the needles were found to be of a different phase.

4.2.6 Ionpairing studies

In the glove box, about 1 mg of a [1.1]ferrocenophane was transferred to a 1 mm Helma cuvette (No. 220-QS). The cuvette was sealed with a Wilmad/omnifit valve assembly (OFV) (Figure 4.3) and removed from the glovebox. Usually 1 ml of freshly prepared solvent was added with a syringe, and a reference spectrum was collected. Usually 5 µl 2.0 M n-BuLi in hexane was added. The cuvette was held at different temperatures during the ion formation. The temperature depended on the solvent used for the experiment. Usually the temperature was 0°C as in the case of *e.g.* DME. If the ion formation was slow at 0 °C, the cuvette was warmed gently with water to room temperature, as with DEE. For the preparation of sodium, potassium and cesium salts of **1**, n-BuNa, n-BuK, MeK and MeCs were used.[5]

The cuvette was inserted in the cryostat and the temperature was lowered in steps to the freezing point of the pure solvent and sometimes lower. Usually, the effect of freezing point depression made it possible to go below the freezing point of the pure solvent. The sample was then in steps brought to room temperature while observing the reversibility of the spectral changes.

UV-vis spectrophotometry was also used for kinetic investigations of the metallation of **1**, **3a** and **3b** in order to evaluate conditions for carbanion formation.

5 Results and discussion

This section is divided into two parts. First a section presenting and discussing our results concerning the nature and mechanism of reactions of [1.1]ferrocenophanyl alkali metals. The second part of this section will present and discuss our results concerning the conformational properties of [1.1]ferrocenophanes.

5.1 Alkali metallation

The incomplete mechanistic model suggested from earlier investigations,[3-5] is one in which the initial state of **2**, with n solvent molecules ligated to lithium ($\mathbf{2_n}$), is in a pre-equilibrium with an intermediate ($\mathbf{2_{(n+m)}}$), with m extra solvent molecules. The rate limiting step, the proton jump, then takes place in the intermediate $\mathbf{2_{(n+m)}}$. Then m solvent molecules leave the intermediate $\mathbf{2_{(n+m)}}$ and the initial state $\mathbf{2_n}$, is regained. This model generates several important questions.
What does the initial state look like; is it aggregated; how many solvent molecules per lithium; where is the lithium located; are we dealing with CIPs or SSIPs? What about the transition state; is there only one solvent molecule extra in the TS, how does the lithium move between carbons 1 and 12?

Answers to some of these questions are presented below.

5.1.1 Ionpairs - studied by UV-vis spectroscopy

UV-vis spectroscopy has been used to study ionpairing in solutions of [1.1]ferrocenophanyl alkali metal salts. Two broad bands, A and B are observed (Figure 5.1). Band A is found in the 400 to 430 nm interval and band B is in the 530 to 600 nm interval. These bands show solvent, temperature and cation dependence.

Figure 5.1 shows spectra of **2** in THF. Absorption maxima of the two bands occur at 409 nm (Band A) and 546 nm (Band B) at +25 °C. The ratio of the absorbance of these two maxima, Abs_A/Abs_B, is 1.4. Upon lowering the temperature to -100 °C, only small changes were observed. The maxima shifted slightly to lower frequencies. The absorbance ratio diminished slightly to 1.2. The colour of the solution remained burgundy red all through the 125 °C interval.

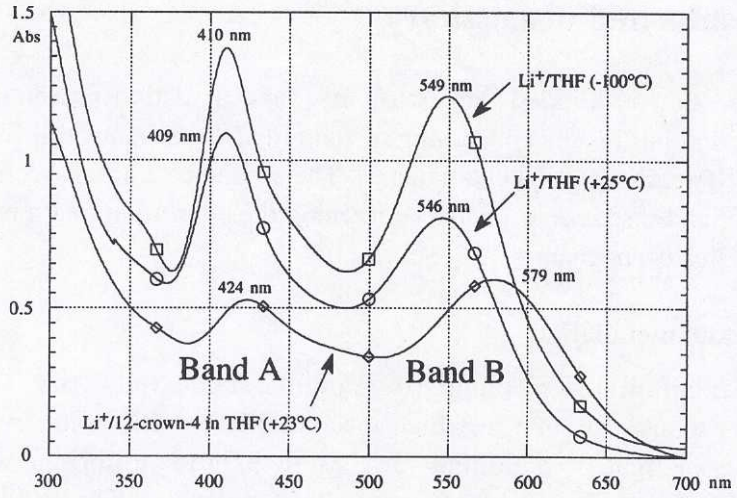

Figure 5.1. Typical appearance of a spectrum of [1.1]ferrocenophanyllithium, in THF at two different temperatures and with 12-crown-4 added.

Upon addition of a strong Li^+ complexing agent, like 12-crown-4, the spectral changes were substantial (Figure 5.1). There was a pronounced red shift of band A and band B by 15 and 33 nm, respectively. The absorbance ratio was inverted: Abs_A/Abs_B = 0.9 and the colour of the solution turned dark bluegreen.

We conclude that the addition of the crown ether had the effect of separating the ions of a contact ion pair, to yield a solvent separated ionpair like state.

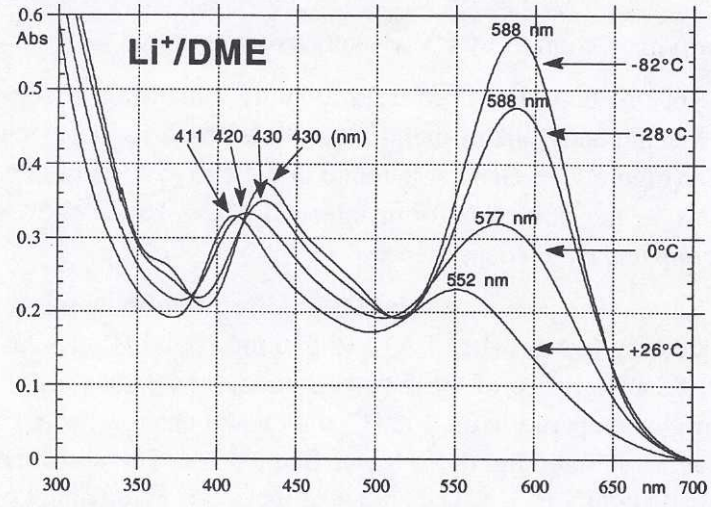

Figure 5.2. The temperature dependence of the UV-vis spectrum of **2** in DME.

The spectrum of **2** in dimethoxyethane (DME) (Figure 5.2) showed a dramatic temperature dependence. At +26 °C, the spectrum was similar to that of **2** in THF: Band A (411 nm), Band B (550 nm), Abs_A/Abs_B = 1.5 and the colour of the solution was also burgundy red. Upon lowering the temperature to -82 °C, there was a pronounced red shift similar to that observed upon addition of 12-crown-4 in THF. The shifts of the bands A and B were 19 and 38 nm, respectively. The absorbance ratio was inverted to 0.7 and the colour of the solution turned dark bluegreen.

These effects of temperature and solvent, are similar to those found by Hogen-Esch and Smid concerning the identification of solvent separated ionpairs (SSIP) and contact ionpairs (CIP).[39,40] We conclude that upon lowering the temperature, the ionpair equilibrium shifts from mainly CIP to mainly SSIP in DME. An important note is that it is normally not possible to distinguish between SSIP and free ions with this method.

Further observations with other solvents and cations (Cs^+ and K^+), are presented in Table 5.1 and Figure 5.3.

Table 5.1. Collection of UV-vis spectral data for some solvent/gegenion combinations together with assignments of dominating type of ionpair.

Solvent/ gegenion	Temp. /°C	Abs_A /nm	Abs_B /nm	ΔA^a /nm	ΔB^b /nm	Abs_A/ Abs_B	Dominating type of ionpair
DEE/Li^+	+25	401	533			1.7	CIP
DEE/Li^+	-116	403	537	+2	+4	1.5	CIP
DMTHF/Li^+	+25	401	536			1.7	CIP
DMTHF/Li^+	-114	405	538	+4	+2	1.4	CIP
THF/Li^+	+25	409	546			1.4	CIP
THF/Li^+	-100	410	549	+1	+3	1.2	CIP
DME/Li^+	+23	411	550			1.5	CIP
DME/Li^+	-82	430	588	+19	+38	0.7	SSIP
THF/12-crown-4/Li^+	+23	424	579			0.9	SSIP
THF/12-crown-4/Li^+	-100	429	585	+5	+6	0.7	SSIP
DEE/Cs^+	+16	422	584			0.9	CIP
DEE/Cs^+	-104	416	580	-6	-4	0.8	CIP

[a] Δ nm A = (Abs_{max} Band A at low temperature) - (Abs_{max} of band A at high temperature) in the same solvent.

[b] Δ nm B = (Abs_{max} Band B at low temperature) - (Abs_{max} of band B at high temperature) in the same solvent.

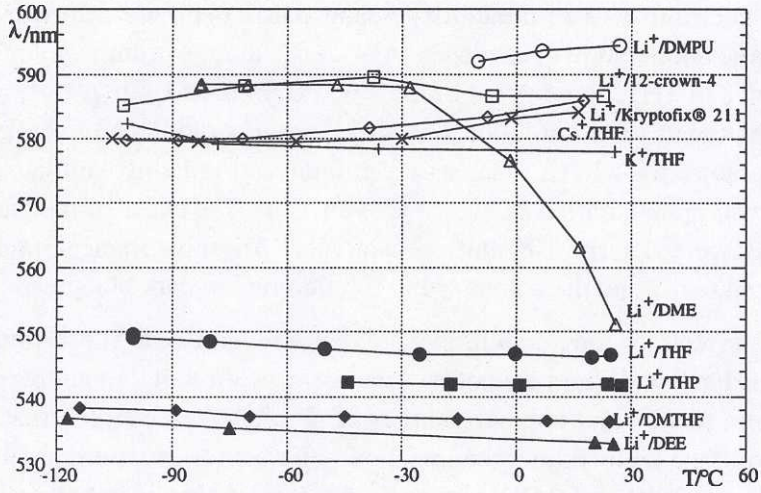

Figure 5.3. Plot of band B absorption maxima versus temperature for [1.1]ferrocenophanyl alkali metal salts, in different solvents.

There are two different interpretations of these results. One is that there is an equilibrium between different species, *i.e.* CIP, SSIP and free ions. The other is that of a gradual change in inter ionic distance with changing solvation caused by change in temperature, solvent polarity and bulkiness of the solvent. The latter explanation seems to fit the spectroscopic data for **2** in THF, DMTHF and DEE, while the first explanation seems to agree with the temperature dependence of **2** in DME. The larger gegenions like, K^+ and Cs^+, show spectra similar to those of SSIPs, although they are most likely CIPs.

Using DNMR spectroscopy, it is possible to reach the slow exchange region for the 1,12 proton transfer in THF. A plot of log k versus 1/T is not curved, which indicates that there is no dramatic change of the initial state in this solvent. In DME it is not even possible to freeze out this process, it seems to be relatively faster at lower temperatures. This is consistent with a change in the initial state, *i.e.* formation of the more reactive SSIP. The bidentate nature of DME seems to favour the formation of more reactive species, *e.g.* SSIPs.

UV-vis studies suggest that although there is an indication of lengthening of the inter ionic distances in going from DEE to THF, there is not a significant fraction of SSIPs in the initial state. The main reason for the rate difference of the lithiation reaction in **2** in these media, seems to be due to the steric differences.

5.1.2 The aggregation state - studied by multinuclear NMR spectroscopy.

The ^{13}C-^{6}Li coupling pattern studied by ^{13}C NMR spectroscopy gave information about the aggregation state of **2**. The isotopically labelled compound [1-^{6}Li]-[1,12-$^{13}C_2$]-[1.1]ferrocenophanyllithium (**^{13}C-^{6}Li-2**) made from [1,12-$^{13}C_2$]-[1.1]ferrocenophane (**^{13}C-1**) and [1-^{6}Li]-n-butyllithium[5] was studied with multinuclear 1D NMR spectroscopy at various temperatures. The synthesis of **^{13}C-1** is described above in section 4.2.2. In the ^{13}C NMR spectrum of **^{13}C-^{6}Li-2** in DMTHF the signal from the carbanionic carbon appeared as a 1:1:1 triplet due to ^{6}Li coupling (^{6}Li is a spin 1 nucleus). This proves that the initial state of **2b** is *monomeric* in DMTHF solution and that the lithium ion is coordinated to the carbanionic bridge carbon in this solvent (Paper I). If aggregates had been present, rather than the monomer, a signal with larger multiplicity would have been observed.

The above observed triplet was observed with a 9.395 T NMR magnet (400 MHz ^{1}H resonance). The coupling constant $J(^{6}Li$-$^{13}C) = 4.0$ Hz, which is small for a monomer. Monomers usually have coupling constants around 15 Hz.[87,88] Attempts were made to observe coupling in DEE using a 11.744 T NMR magnet (500 MHz ^{1}H resonance), but only a broad carbanion carbon signal was observed. This is probably due to the higher quadrupole relaxation rate of the ^{6}Li nucleus at this higher field. No resolved triplet could be recorded for **2** in DMTHF at the higher field either. An interesting observation was that samples that were not freshly made, *e.g.* stored in the freezer in an argon filled plastic bag over night, had a significantly smaller linewidth than when freshly made. It was also noticed that a considerable portion of **2** had quenched. Addition of more n-BuLi did not cause the carbanion signal to broaden despite the increased concentration of **2**. This may be the effect of the decomposition of the solvent by **2** and n-BuLi. The alkoxides that are the result of such reactions probably participate in ionpairing and aggregation formation that lead to intermolecular exchange of the lithium. In THF, no broadening of the carbanion signal due to ^{13}C-^{6}Li coupling could be detected.

5.1.3 The solid state structure of [1.1]ferrocenophanyllithium

Attempts to crystallise **2** in THF have so far only led to conglomerates of small crystals that have not been suitable for X-ray analysis. However, we have managed to get sufficiently good crystals of **2** in DMTHF to be able to obtain solid state structural data (Figure 5.4) (Paper II).

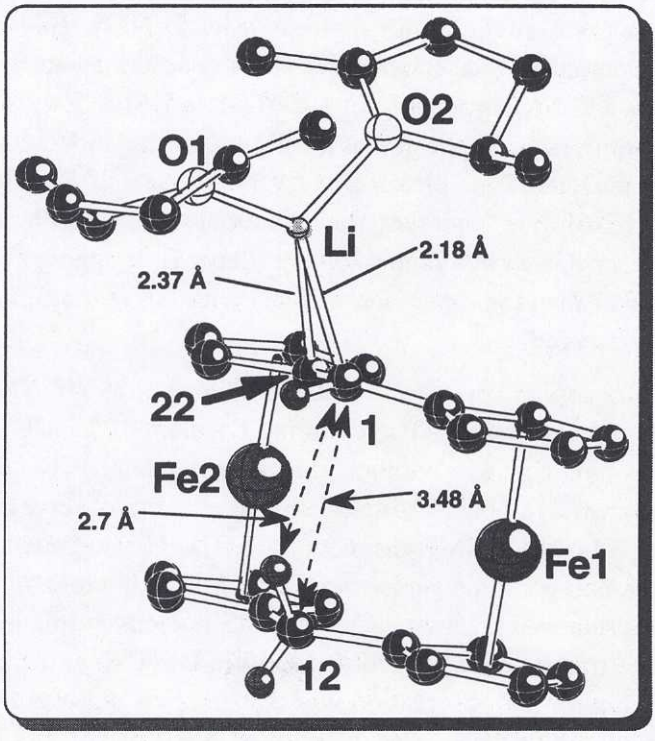

Figure 5.4. The solid state structure of **2** in DMTHF.

Compound **2** is a monomer in the solid state as well. The lithium ion is coordinated to two solvent molecules, C1 and C22 (*i.e.* tetracoordinated). Carbon C1 is somewhat closer (2.18 Å) than C22 (2.37 Å) to lithium. The Li^+ is located in an *exo* position. The $[C\cdots H\cdots C]^-$ hydrogen bond proposed earlier, by Mueller-Westerhoff and coworkers, is not present in the solid state. The "lone pair" hybrid at C_1^- points away from *endo* H_{12} and the relatively large distances between C_1^- and *endo* H_{12} (2.7 Å) shows that there is no hydrogen bond in the solid state. The C_1^- to *endo* H_{12} distance is close to the van der Waals radii of hydrogen and a carbanionic carbon. The mechanistic implications of an *exo* positioned Li^+ will be dealt with later (*vide infra*).

5.1.4 Solvent and other complexing agents - their roles

The change of solvent or addition of small amounts of other complexing agents, is by far the most frequently used route to improvement in synthetic alkali metallation chemistry. Yet, it is hard to study specific solvent effects, simply because it is hard to change the concentration of the bulk solvent. We have changed the solvation of lithium by adding complexing agents such as 12-crown-4 and kryptofix® 211, which create a SSIP like state. The expected result would be an increase in the rate of the intramolecular lithiation reaction. However, there is only a slight increase in the rate,[5] possibly due to steric reasons. The inter ionic distance is increased in the initial state, but the size of the lithium/12-crown-4 complex make rearrangements more difficult, since extra solvation by the solvent is sterically improbable.

The interest lies in elucidating the mechanistic role of common solvent molecules such as DEE, THF and DME. With the [1.1]ferrocenophanyl alkali metal salts we have a unique possibility. The intramolecular lithiation in **2** shows a large solvent dependence (Table 5.2).

Table 5.2.[a] Rate constants for the intramolecular rearrangement in [1.1]ferrocenophanyl alkali metal salts in different solvents and at different temperatures.

Gegenion	Temp./°C	Exchange region	Solvent	Rate constant of the proton jump/s^{-1}
Li^+	21	fast	THF	32000
Li^+	21	fast	THP[b]	2400
Li^+	21	fast	DME	-
Li^+	21	fast	MTHF[b]	9500
Li^+	21	slow	DMTHF	10
Li^+	23	slow	DEE	8
Li^+	-100	slow	THF	63
Li^+	-100	slow	THP[b]	2.3
K^+	-9	fast	THF	26000
K^+	-100	slow	THF	76
K^+	-10	fast	DME	28000
K^+	-95	slow	DEE	12
Cs^+	-103	slow	THF	23
Cs^+	-20	fast	THF	73000

[a] from the Thesis of Ö. Davidsson[5]

[b] THP = tetrahydropyran, MTHF = 2-methyltetrahydrofuran

In THF, the lithiation reaction is about 4000 times faster than in DMTHF. This suggests that it is possible to catalyse the reaction by THF in DMTHF. To find out the reaction order, we titrated a solution of **2** in DEE or DMTHF with THF. The reaction rate was measured using DNMR spectroscopy. The results are displayed in Figure 5.4. For experimental details see section 4.2.4.

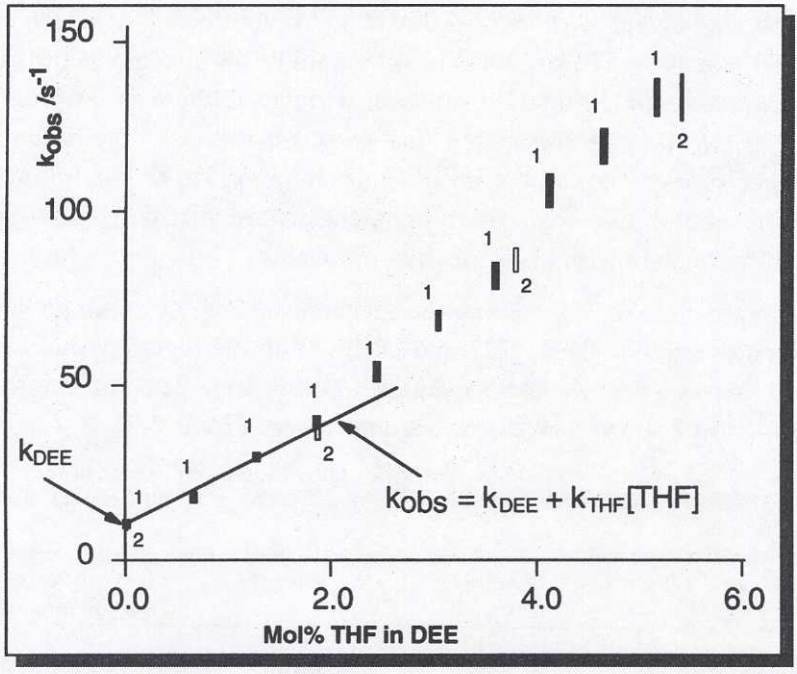

Figure 5.5. Plot of the observed rate constant for the intramolecular lithiation of **2** in DEE versus the mol% of THF. The results obtained with two different solutions of **2**, labelled 1 and 2. The size of the markers indicate estimated maximal errors, due to errors in rates, THF concentration and temperature.

The linear dependence of the observed rate constant on the mol% THF up to 2 mol% THF shows that the catalysis is first order in THF at low concentrations. Thus, the rate limiting transition state contains one solvent molecule more than the initial state (Paper III). A qualitative catalysis experiment with DME instead of THF indicates a different behaviour. After a large initial rate enhancement, a plateau of rate constant versus mol% DME is reached. This indicates that DME is replacing DEE molecules in the initial state first. At ca 1.5 mol% DME the rate increases dramatically again. This could be due to the formation of SSIPs or that only two DME molecules are involved in the TS. The difference in behaviour is most likely due to the bidentate nature of DME.

Reactions with solvents

The alkali metal reagents we use reacts with the ferrocenophane as well as the solvents. These side reactions produce alkoxides that may interfere with the mechanistic studies of the rearrangement in the [1.1]ferrocenophane alkali metal salts. Side reactions with the solvent becomes more important with stronger bases; MeLi < n-BuLi < n-BuNa < n-BuK < n-BuCs and more polar solvents. In order to suppress these side reactions, it is possible to use weaker bases and/or lower temperatures for production of carbanions. This, however, means longer exposure time of the solvent to the base. compound **2** seems to be basic enough to metallate THF at room temperature.

A breakthrough regarding this problem is the crystallisation of **2** in DMTHF, which yields purer samples.

5.1.5 A detailed mechanism of the alkali metallation reaction

A detailed mechanism, that we have proposed based on our investigations, is presented below.

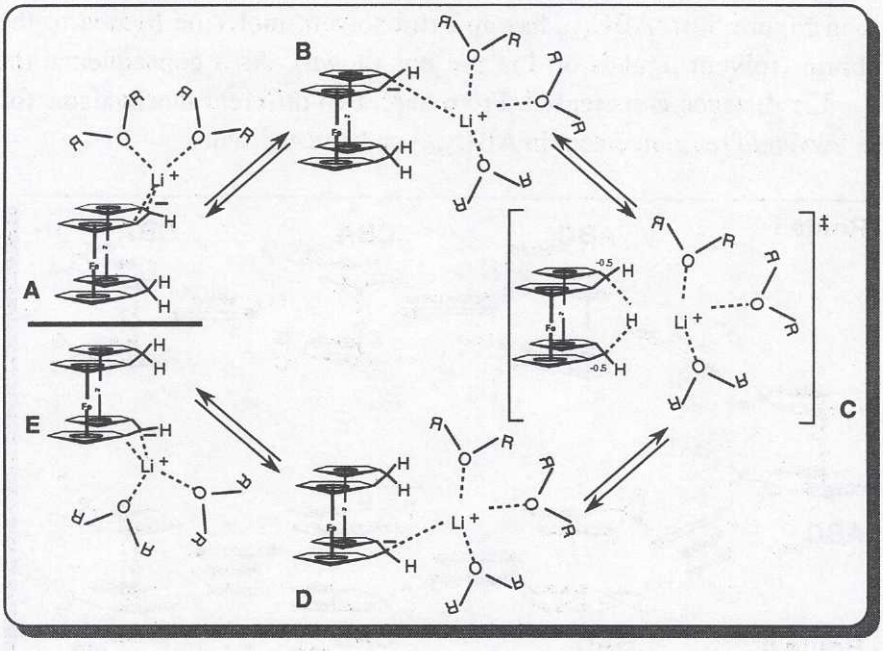

Figure 5.6 Our proposed mechanism for the intramolecular lithiation in **2**.

The mechanism presented in Figure 5.6 involves the following events:

1. In the initial state **2** is a monomer and a CIP with two solvent molecules ligated to the lithium ion (A in Figure 5.6).
2. From A, an intermediate is formed with an extra solvent molecule ligated to the lithium, and thereby increasing the $C_1^-\cdots Li^+$ distance (B).
3. In the alkali metallation TS, the proton is in the middle between the carbons 1 and 12 (C).
4. The intermediate is reformed with the carbanionic carbon being C_{12}^- and where the lithium ion and proton have moved to the opposite carbon bridge, respectively (D).
5. The intermediate loses the third solvent molecule and the initial state is reached again (E).

One step in this mechanism is not clear, and that is the rearrangements of the ligated lithium ion. If the solid state structure is similar to the initial state structure in solution, then Li^+ has to move from an *exo* position at C_1 to an *exo* position at C_{12} in this lithiation reaction. Below, we propose two possible mechanisms for this motion.

In Figure 5.7, an intermediate ABC_{exo} is formed from the initial state of **2** (A in Figure 5.6). ABC_{exo} has an extra solvent molecule ligated to the lithium (solvent ligands on Li^+ are not shown). As a consequence the $C_1^-\cdots Li^+$ distance is increased. From here, two different mechanisms for the *exo/endo* rearrangement in ABC_{exo} can be visualised.

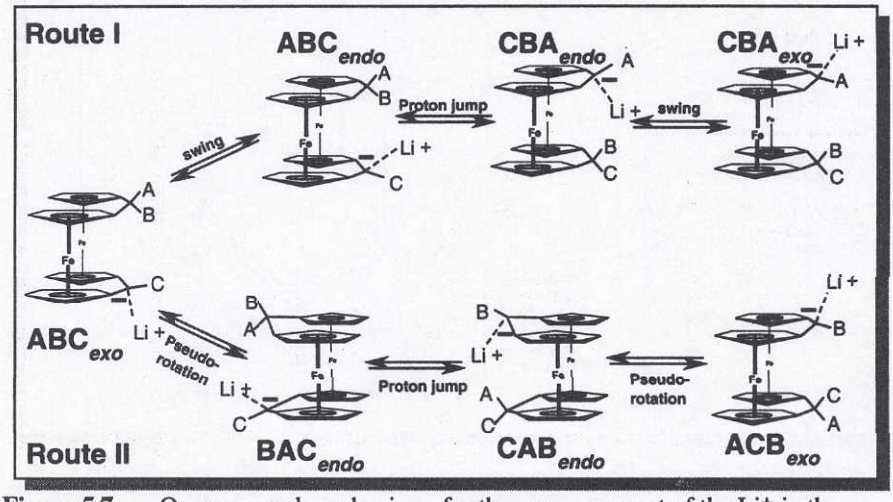

Figure 5.7 Our proposed mechanisms for the rearrangement of the Li^+ in the lithiation reaction in **2**.

Route I

In the intermediate ABC_{exo}, the complexed Li^+ may "swing", approximately perpendicular to the C_1-C_{22} bond, from the *exo* position to an *endo* position (ABC_{endo}). In the ABC_{endo} intermediate, the alkali metallation takes place and proton B "jumps". The intermediate CBA_{endo} is formed with the complexed lithium in an *endo* position at the C_{12}, followed by the formation of CBA_{exo} with a lithium "swing".

Looking at the overall reaction, from ABC_{exo} to CBA_{exo}, the C and A protons exchange and the B proton jumps.

Route II

The intermediate ABC_{exo} performs a pseudo-rotation or ring-inversion which brings the *exo* positioned Li^+ into an *endo* position at the same carbon and exchanges the A and B protons (BAC_{endo}). In the BAC_{endo} intermediate, the alkali metallation takes place and proton A "jumps". The intermediate CAB_{endo} is formed with the complexed lithium in an *endo* position at the C12. This is followed by a pseudo-rotation or ring-inversion which results in the intermediate ACB_{exo}. In this last process, the A and C protons exchange.

Looking at the overall reaction, from ABC_{exo} to ACB_{exo}, the B and C protons exchange and the A proton jumps.

In the catalysed reaction of **2**, complete band shape analysis of the singlet and the triplet results in different rate constants.[89] The singlet is the signal from the proton at the carbanionic carbon and the triplet is the signal from the "jumping" proton. We obtain a larger rate constant from the triplet than from the singlet.

5.2 Conformational studies of [1.1]ferrocenophanes

This section first presents a mechanistic model for the conformational behaviour of [1.1]ferrocenophanes, based on a comparison between the cyclohexane system and the [1.1]ferrocenophane system. This is followed by results and discussion sections dealing with [1.1]ferrocenophane, 1,12-dimethyl-[1.1]ferrocenophane and a special section for comparison of X-ray structures.

5.2.1 The conformational space of [1.1]ferrocenophanes, a comparison with cyclohexane.

During our investigations of this group of molecules, we have found that an analogy between the [1.1]ferrocenophane system and the cyclohexane system is useful for explaining the conformational behaviour of [1.1]ferrocenophanes.

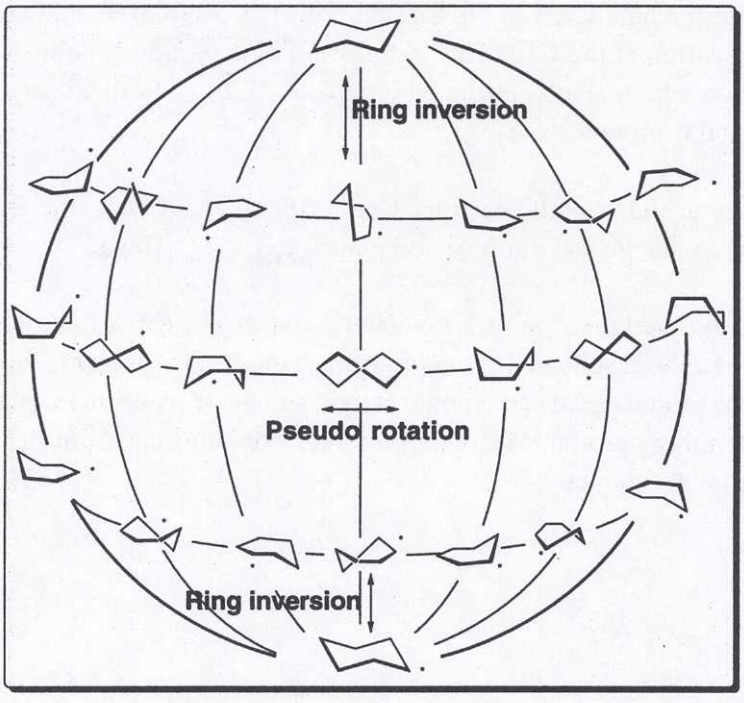

Figure 5.8. The conformational globe of cyclohexane.

The cyclohexanes are among the most well known and investigated classes of compounds in chemistry.[51,90-95] Already in 1890, H. Sachse pointed out the geometrical properties of six methylenes combined in a ring.[94] He understood that two principal forms could be formed, the boat form and the chair form, and he also pointed out that the boat form would be extremely flexible and the chair form would be "rigid".

In addition, he realised that substituents on a cyclohexane could adopt either an axial or an equatorial position. It took until the 1930's, before the existence of the chair form was established and it took another 20 years before other forms of cyclohexane were experimentally observed.

Many scientists have concerned themselves with the conformational properties of cyclohexane, both experimentally and theoretically (see Cremer and Szabo[93] and references therein). Many ways to visualise the conformational space of cyclohexane have been developed of which one of the best can be seen in Figure 5.8.

To see the analogy between the [1.1]ferrocenophane and cyclohexane systems, there are some common structural elements that has to be pointed out. Consider the boat conformer of cyclohexane and the *syn*-conformer of [1.1]ferrocenophane, it becomes apparent that the bow and stern carbon atoms in cyclohexane (atoms 1 and 4 in Figure 5.9a) are analogous to the bridge methylene carbon atoms in [1.1]ferrocenophane (atoms 1 and 4 in Figure 5.9b).

Secondly, the other carbon atoms in the cyclohexane ring (atoms 2, 3, 5 and 6 in Figure 5.9a) are then analogous to the dummy atoms which are placed in the centre of gravity of the cyclopentadienyl moieties (atoms 2, 3, 5 and 6 in Figure 5.9b).

It should be pointed out that [1.1]ferrocenophane does not have as high a symmetry as cyclohexane, and that for simplicity the comparison is always made between boat and *syn* structures and chair and *anti* structures and not the, in some cases, more energetically stable twist forms (see *e.g.* Table 5.3).

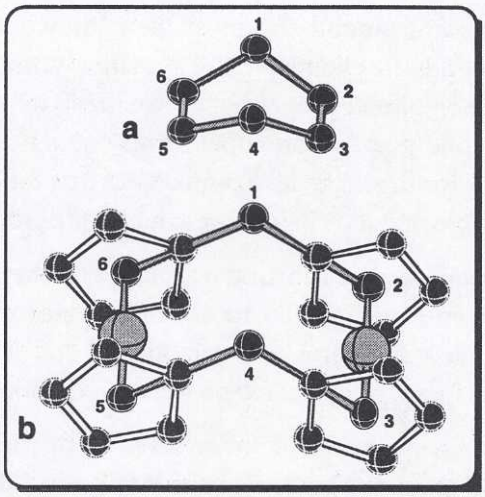

Figure 5.9. Structure elements that are common to both cyclohexane and [1.1]ferrocenophane. The dihedral angles used in the calculation of the pseudo-rotation are defined from structure b. ω_{1234} is defined by the atoms 1, 2, 3 and 4. The other angles are defined in a similar manner.

The extent of this analogy is especially clear from Figure 5.10 where a comparison is made between 1,12-dimethyl[1.1]ferrocenophane (DMFCP) and 1,4-dimethylcyclohexane. Consider *e.g. exo,exo,syn*-DMFCP (syn *c.f.* boat) which is analogous to boat-1(e),4(e)-dimethyl-cyclohexane (e = equatorial). It is well known that boat-1(e),4(e)-dimethyl-cyclohexane can inter convert into boat-1(a),4(a)-dimethyl-cyclohexane (a = axial) *via* pseudo-rotation (or ring-inversion), and the same mechanistic pathways may also open to *exo,exo,syn*-DMFCP whereby it becomes *endo,endo,syn*-DMFCP.

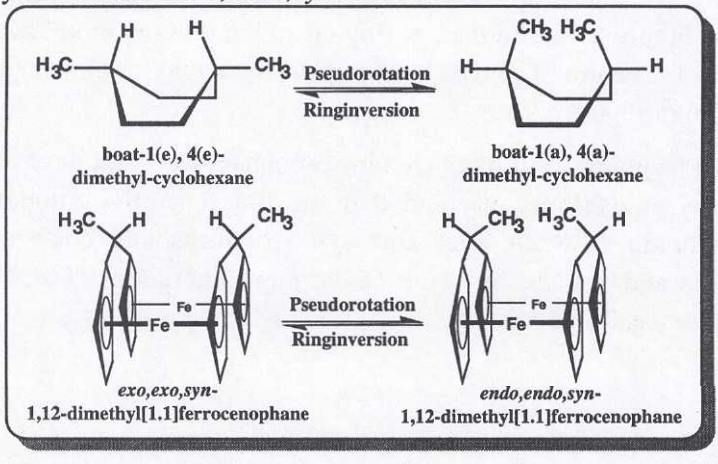

Figure 5.10. An example of the common conformational properties of cyclohexane and [1.1]ferrocenophane.

At this point, we can create the conformational space of [1.1]ferrocenophane, Figure 5.11.

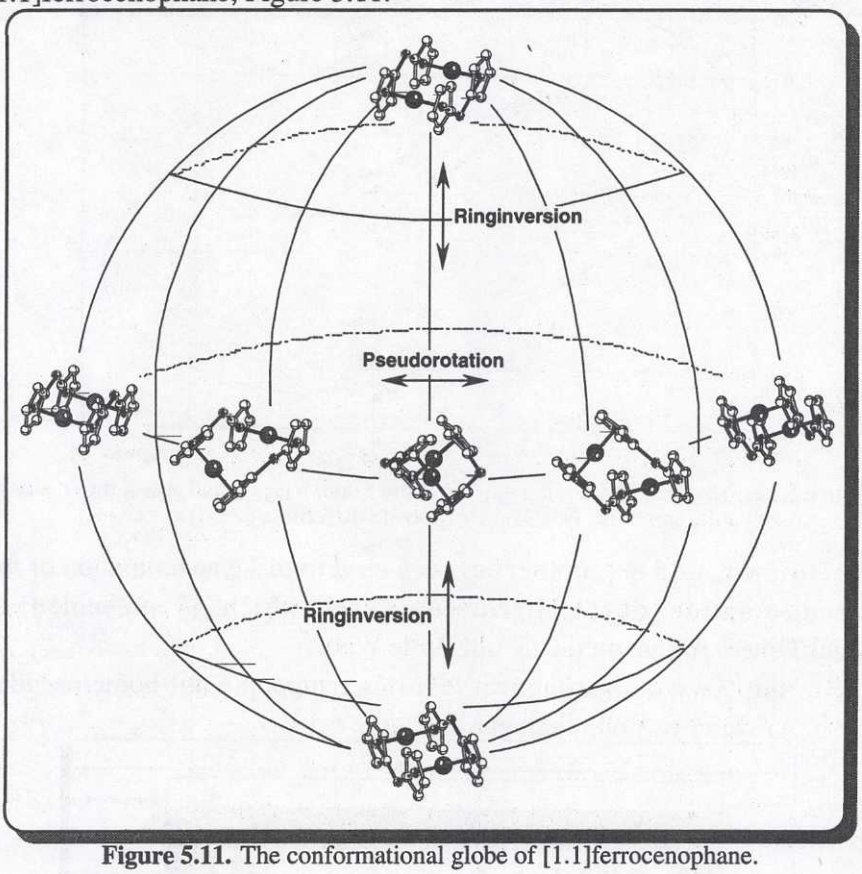

Figure 5.11. The conformational globe of [1.1]ferrocenophane.

Another attempt to visualise the conformational properties of [1.1]ferrocenophane, has been to mathematically describe the pseudo-rotation in **1**. This has been done previously for six membered rings (see Cremer and Szabo[93] and references therein), but all these works have focused on the total description of the conformational space of these six (and higher) membered rings, which invariably has led to the transfer to coordinate systems with low intuitive value. The mathematical model that we present in this work,[96] is based on the internal coordinates (bond lengths, bond angles and dihedral angles) of [1.1]ferrocenophane and uses a dihedral angle as the driving variable for the pseudo-rotation. Figure 5.12 show a graph over a part of the solution space of a pseudo-rotation for the ideal C_{2v} [1.1]ferrocenophane, expressed in the dihedral angles ω_{1234}, ω_{3456} and ω_{2345}. The dihedral angles refer to the structure in Figure 5.9b.

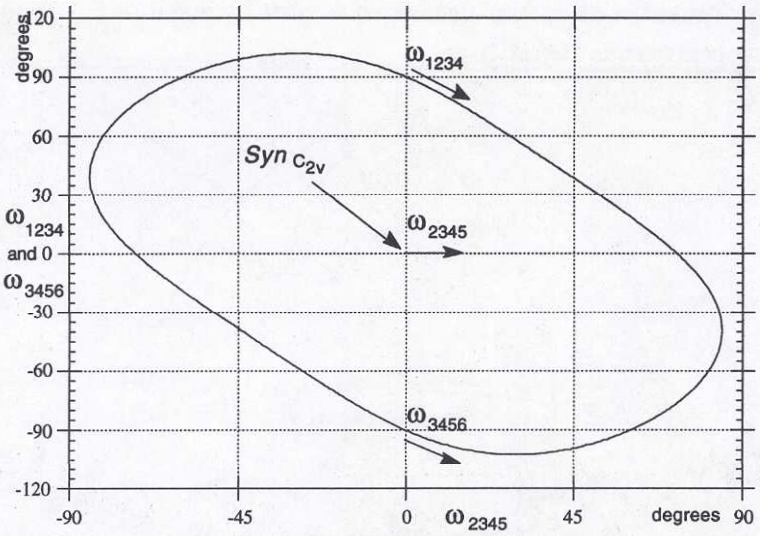

Figure 5.12. ω_{2345} is the driving angle (on the x-axis). ω_{1234} and ω_{3456} move along the same line however in opposite directions ($\omega_{1234} = -\omega_{3456}$).

This mathematical description has been used to make an animation of the pseudo-rotation of [1.1]ferrocenophane, which is presented in QuickTime® format on the World Wide Web.
(URL: http://www.che.chalmers.se/inst/oc.gu/people/jml-home/pseudo-fcp-movie.html.). A clip is shown in Figure 5.13.

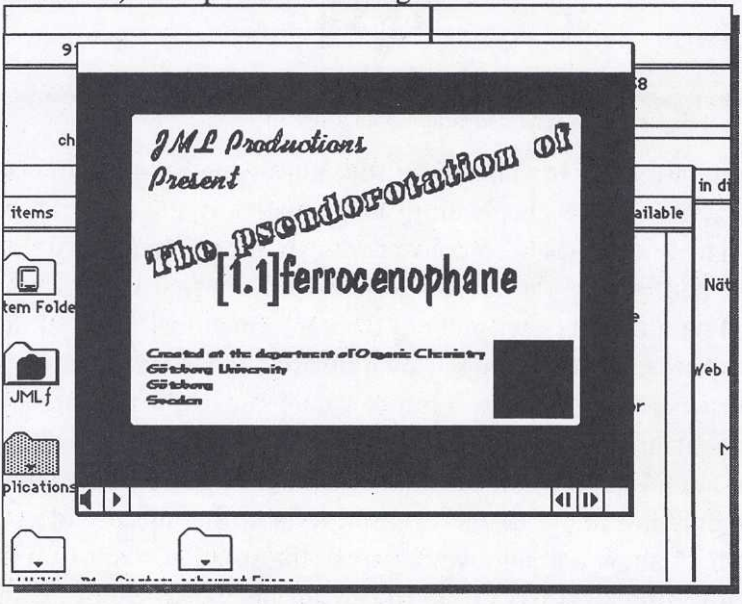

Figure 5.13. A clip from the animation of the pseudo-rotation of [1.1]ferrocenophane, accessible via WWW (www.che.chalmers.se)

5.2.2 [1.1]Ferrocenophane - a molecular acrobat

Although a degenerate inter conversion of **1** (Figure 5.14) has been proposed[7] as the reason for the simple NMR spectrum, there has been no proof for this. We have been able to freeze out this internal inter conversion on the NMR time scale (500 MHz), and thereby proving that there is indeed an internal degenerate inter conversion and not accidental chemical shift equivalence (Paper IV). Furthermore, we could determine the Gibbs free energy of activation from the coalescence temperature (-123 °C) to 28 ± 4 kJ mol^{-1}. The mechanism with which this degenerate interconversion takes place, is either pseudo-rotation or ring-inversion as outlined in the preceding section. Studies of the mechanical models show that pseudo-rotation seems to be the most likely mechanism since only bond rotation is involved and no bond angle bending as in the ring-inversion mechanism. But, there is no experimental proof whatsoever and the ring-inversion mechanism can not be excluded. So far, only *syn*-type conformers of **1** have been isolated in the solid state (see section 5.2.4).[12,Paper V] An *anti*-type conformer of **1** has to be postulated in the ring-inversion mechanism. Our attempts to use solid state NMR to find out if there are any *anti*-conformers of **1** are inconclusive. The NMR spectrum show two sets of signals for **1**, but they may well be derived from the different crystal phases of **1**.

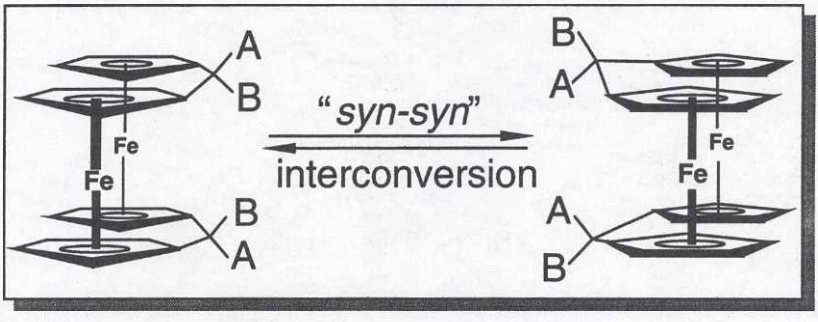

Figure 5.14. A degenerate inter conversion of **1**, showing the exchange of the *exo* and *endo* positions. The α', α" protons and β', β" protons also exchange simultaneously.

5.2.3 1,12-Dimethyl-[1.1]ferrocenophane - novel isomers

At first glance there are eight structures of DMFCP, with respect to the position of the bridges (*syn* or *anti*) and to the position of the methyl groups (*exo* or *endo*) (Figure 5.15).

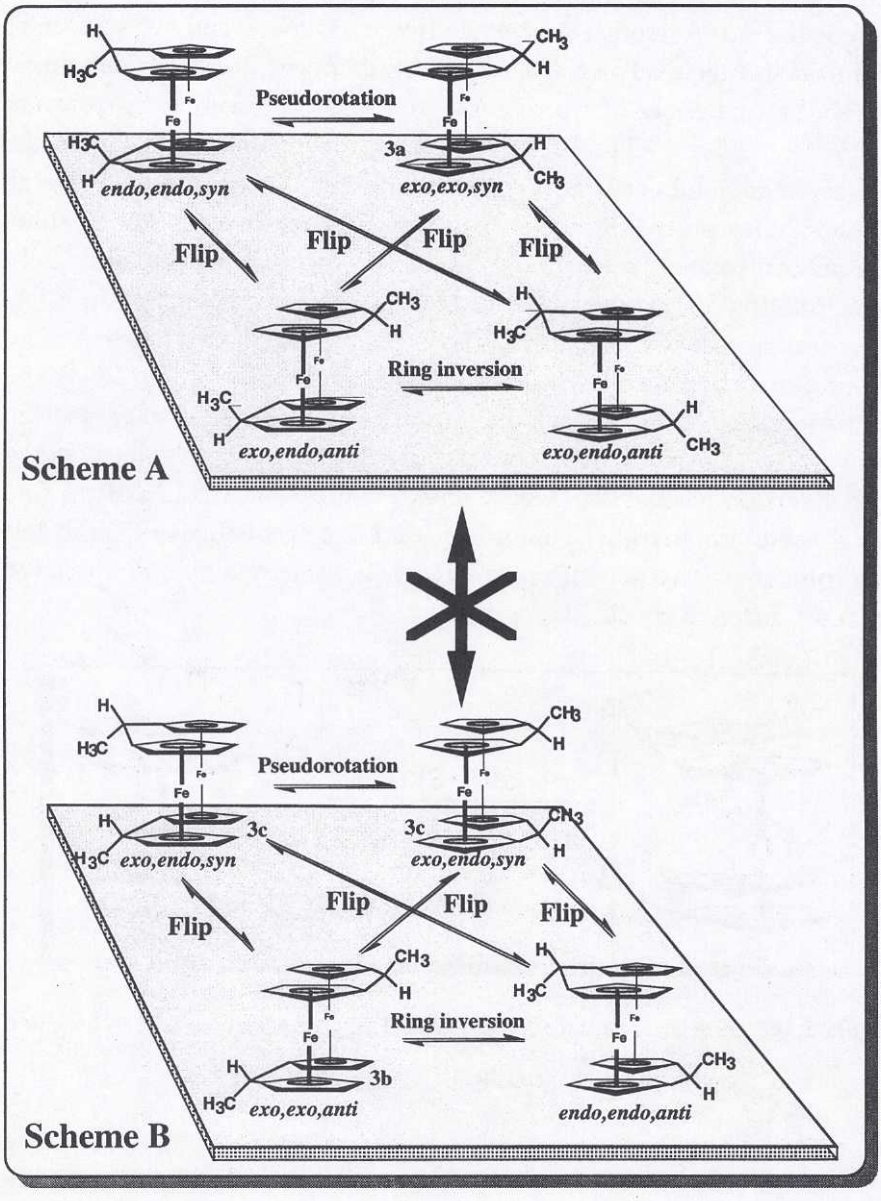

Figure 5.15. The six diastereoisomers of 1,12-dimethyl-[1.1]-ferrocenophane and their inter conversion pathways.

However, of these eight structures, there are two pairs of identical structures, *exo,endo,anti*-DMFCP (scheme A) and *exo,endo,syn*-DMFCP (**3c**, scheme B), which are connected *via* ring inversion and pseudo-rotation respectively. This leaves six possible diastereoisomers of DMFCP.

Figure 5.15 depicts these diastereoisomers as well as their inter conversion pathways. For simplicity, the comparison is always made between boat and *syn* structures and chair and *anti* structures and not the, in some cases, more energetically stable twist forms (see Section 5.2.4). Furthermore, if a twist is introduced in the diastereoisomers, the complexity increases since there will be enantiomeric pairs of each structure. The enantiomers are formed from clockwise and anticlockwise twists, relative to the eclipsed (C_{2v}) diastereomer (Figure 5.16).

Scheme A in Figure 5.15, shows *exo,exo,syn*-DMFCP (**3a**), *endo,endo,syn*-DMFCP and *exo,endo,anti*-DMFCP which all are conformational isomers *i.e.* they can interconvert without breaking any bonds. Scheme B shows *exo,exo,anti*-DMFCP (**3b**), *endo,endo,anti*-DMFCP and *exo,endo,syn*-DMFCP (**3c**) which are also conformational isomers. The conformers within scheme A and B belong to different configurational isomers, *i.e.* they cannot inter convert unless there is a bond broken (or inversion at a carbon). In Figure 5.15, the term "flip" means a flip of one of the bridge carbons from one side to the other, which is the mechanistic equivalent to half a ring-inversion.

In the synthesis of DMFCP, there are two components in the product according to NMR. One set of signals belongs to **3a**, as has been shown by Watts and McKechnie.[8,97] The other set of signals were, tentatively, assigned to **3c** by Watts and coworkers[10] and later also by Mueller-Westerhoff and coworkers.[11] Mueller-Westerhoff recognised the fact that in order for the structure **3c** to be in accordance with the NMR spectrum, it had to perform a "*syn-syn*" inter conversion.

Out of the overall six diastereoisomers, three have been crystallised so far. The first isomer to be structurally characterised by X-ray diffraction was *exo,exo,syn*-DMFCP (**3a**),[8,9] the second isomer was *exo,exo,anti*-DMFCP (**3b**) (Paper VI) and the third isomer was *exo,endo,syn*-DMFCP (**3c**) (Paper VII).

The structure of **3b** was very interesting since it proved to be the first carbon bridged *anti*-[1.1]ferrocenophane, a conformer thought to be too

structurally rigid and sterically hindered to exist. However, an analysis of the structural features of **3b** showed that tilting in a ferrocene unit allowed steric relief (*vide infra*). Assuming that there is a fast inter conversion between the two enantiomers of **3b** (Figure 5.16), then the C_{2v} type conformer would fit the NMR data previously supposed to be a *syn-syn* interconverting **3c**.

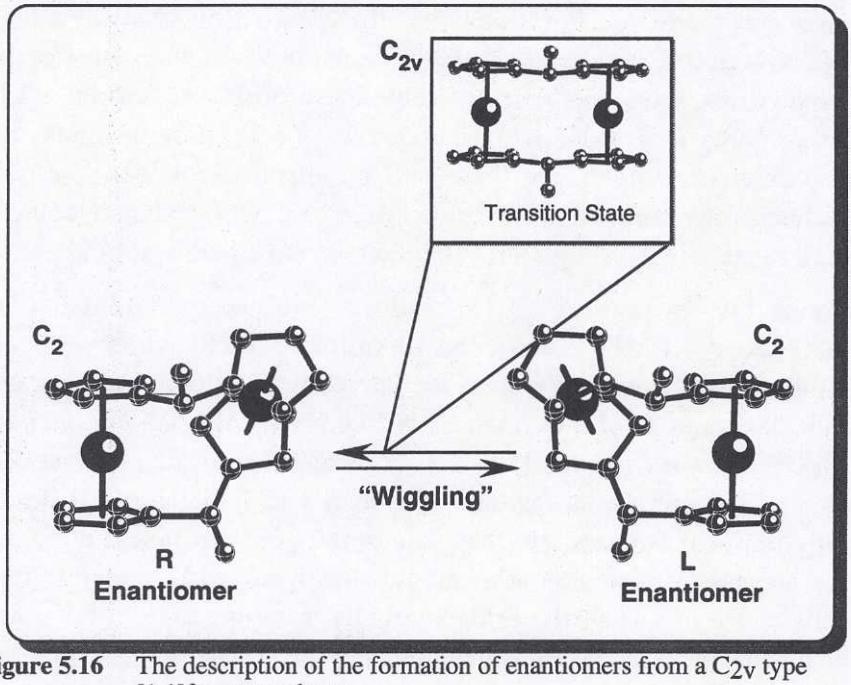

Figure 5.16 The description of the formation of enantiomers from a C_{2v} type [1.1]ferrocenophane.

With the isolation and structural characterisation of **3c**, some interesting facts were gathered.

The NMR spectrum of **3c** in THF indicates a degenerate inter conversion (or accidental chemical shift equivalence) since only six signals can be recorded, *e.g.* only one doublet for the methyl protons at 1.23 ppm. However, whether this inter conversion occurs *via* a pseudo-rotation or *via* ring-inversion with **3b** as an intermediate, is not possible to conclude. The fact that the solution spectrum of dissolved crystals of **3b** is identical with that of dissolved crystals of **3c** indicates that there, at least, exists a ring-inversion pathway with low enough barrier at room temperature.

In order to investigate this interconversion we prepared ^{13}C labelled DMFCP, *i.e.* 1,12-([23,24-$^{13}C_2$]-dimethyl)-[1.1]ferrocenophane (**^{13}C-3**).

Dynamic NMR studies of the isomeric mixture of ^{13}**C-3** are inconclusive, so far, and only show that some exchange process is going on (Figure 5.17).

The ^{13}C signal at 31.8 ppm (peak A) is from the methyl groups of **3a**. The ^{13}C signal at 29.1 ppm (peak B) is from the methyl groups of either **3b** or pseudo-rotating **3c** or **3b** in equilibrium with **3c**. Peak B broadens and disappear at ca -100° C to reappear at -140°C as 2 signals of approximately the same intensity at 33.2 ppm (peak B^1) and 21.2 ppm, (peak B^2).

This is proof of a dynamic process, but it is still not possible to say if it is the pseudo-rotation of **3c** that has been frozen out or if it is the equilibrium between **3b** and **3c**, or possibly both. In the case of the pseudo-rotation of **3c**, the "slow exchange" signals should have appeared symmetrically around the "fast exchange" peak. In the case of an equilibrium between **3b** and **3c**, the relative distances for the "slow exchange" peaks (peaks B^1 and B^2) from the "fast exchange peak" (peak B) indicate that peak B^1 should have twice the intensity of peak B^2. An added complication is that the signal from the methyls in the **3a** isomer, in this sample, may cover a signal from the exo methyl group in **3c**.

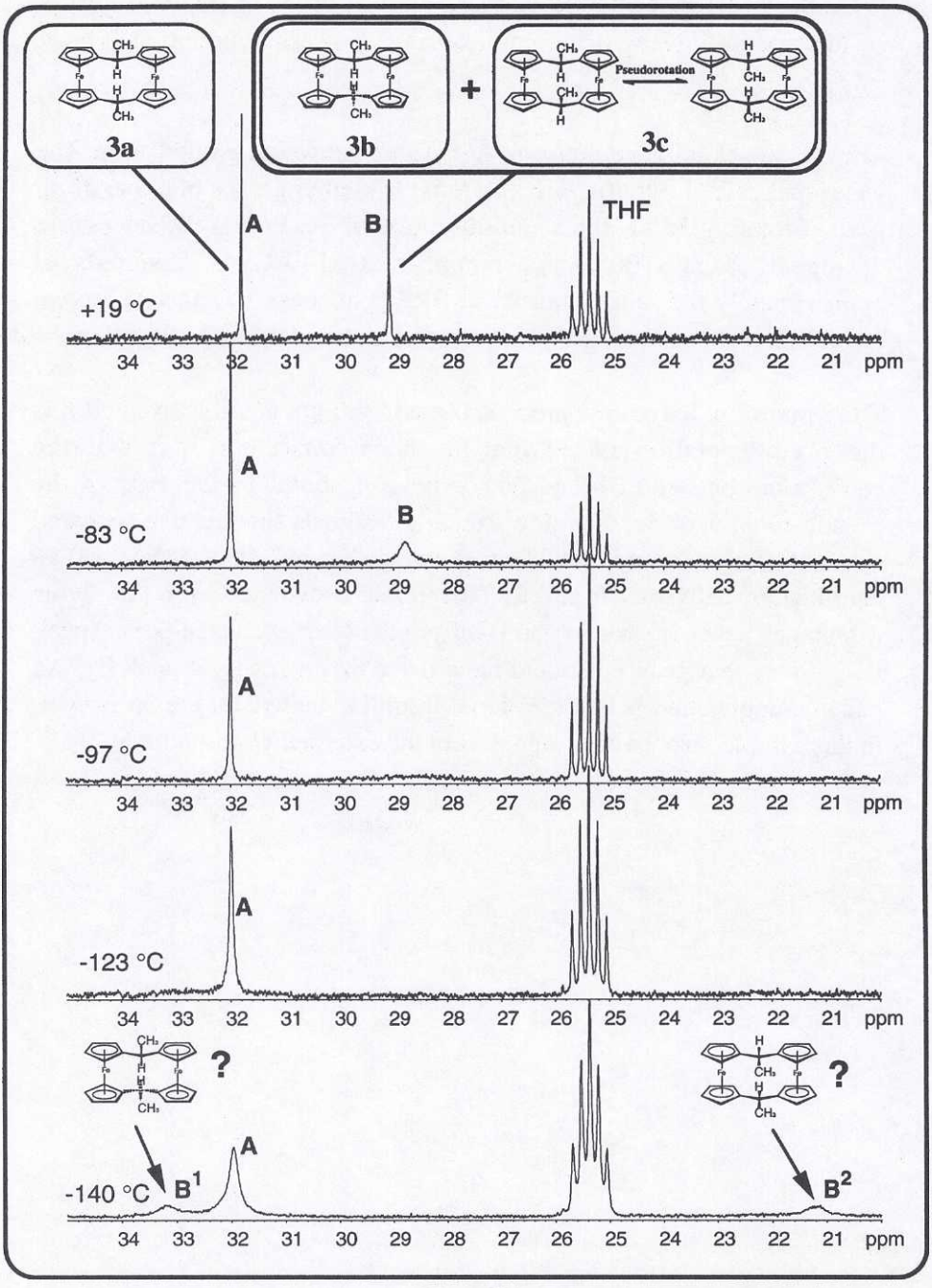

Figure 5.17. Temperature dependence of the ^{13}C NMR spectrum (125 MHz) of **^{13}C-3**. Only the methyl region is shown.

5.2.4 The structures of the novel isomers - a comparison of their X-ray structures

The main structural features of a [1.1]ferrocenophane molecule may be described by four essential angles: the *twist*, the *rotation*, the *tilt*, and the *bridge* angle (see Figure 5.18). The twist angle is defined as the dihedral angle between the best planes of the cyclopentadienyl rings of the *same* organic ligand. The rotation angle is defined by the [C_A-(centre of gravity of ring A)-(centre of gravity of ring B)-C_B] torsion angle, where rings A and B are the cyclopentadienyl rings of one "ferrocene unit". The tilt angle can then be defined as the dihedral angle between the two rings (*i.e.* from different organic ligands) of such a "ferrocene unit." Finally, the bridge angle is defined as the bond angle around the bridging carbon with respect to the two quaternary ring carbons in the same organic ligand. In Table 5.3, these angles are listed for **3a-c** and for the two known phases of **1**.

Table 5.3. The four essential angles in different isomers of 1,12-dimethyl[1.1]-ferrocenophane together with two different forms of [1.1]ferrocenophane and **2** in DMTHF

Isomer	Twist angle (°)	Rotation angle (°)	Tilt angle (°)	Bridge angle (°)
3a (*exo,exo,syn*)[9]	30.2	21.5	3.1	115.8
	31.5	23.9	3.0	117.5
3b (*exo,exo,anti*)[Paper VI]	36.1	3.4	4.1	116.9
	34.0	53.9[a]	22.7	118.1
3c (*exo,endo,syn*)[Paper VII]	39.4	32.0	7.3	117.0
	38.2	31.4	6.2	117.3
1a (*syn*)[12]	13.8	≈10	2.4	121.3
	12.7	≈10	1.4	121.7
1b (*syn*)[Paper V]	1.6	0.5	3.6	121.8
	3.2	0.5	1.2	127.0
2(in DMTHF)[Paper II]	1.8	0.8	1.6	121.7
	2.4	0.6	1.0	122.5

[a]A rotation angle of 53.9° is reasonable only with reference to a [1.1]ferrocenophane molecule, but for a comparison with ferrocene derivatives a value of 18.1° (72-53.9) is the adequate rotation angle. This angle is close to an ideal midpoint (18.0°) between an eclipsed and a staggered conformation.

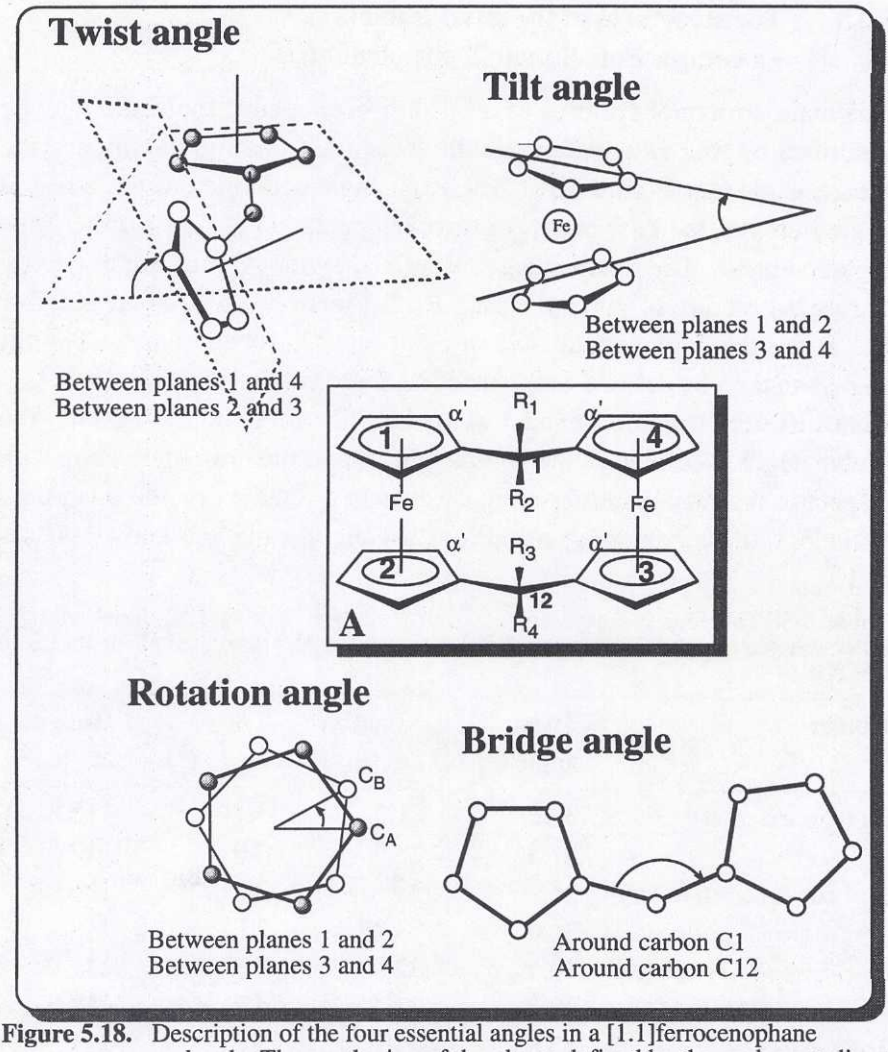

Figure 5.18. Description of the four essential angles in a [1.1]ferrocenophane molecule. The numbering of the planes defined by the cyclopentadienyl moieties are shown in the structure A.

From the data in Table 5.3, some general relationships involving the essential angles can be established (there are a few special exceptions):

1. The bridge angle seems not to be coupled to any other angle.
2. The twist and rotation angles are directly linked as components of a "pure" pseudo-rotation.
3. The tilt angle automatically induces a change in the twist angle which usually, but not always, leads to a change in the rotation angle.
4. The tilt angle is instrumental in the ring inversion mechanism.

Furthermore, the data in Table 5.3 indicates three different mechanisms to relieve internal steric strain in [1.1]ferrocenophane molecules, bearing in mind that packing effects - *i.e.* intermolecular contacts - also will be of significance for the solid state conformation.

The first mechanism involves an opening of the bridge angle in order to reduce H···H intramolecular repulsive interactions of the α' protons. This mechanism is utilised by all the [1.1]ferrocenophanes, but is especially visible in **1b** which exhibits a bridge angle of 122°.

The second mechanism increases the twist and rotation angles, *i.e.* starts a movement along a pseudo-rotation path, which initially results in an increase of the distances between the α' protons in the same organic ligand. In this mechanism, both the twist angles and the rotation angles change in a coupled manner, and it is used by all [1.1]ferrocenophanes with the exception of **1b** (**3b** comprises a special case, *vide infra*).

In the third mechanism, the tilt angle is altered, which seems to be the mechanism with the steepest potential. The effect of tilting is divided into two parts. Firstly, as in the case of **3b** (*exo,exo,anti*), where the *anti* conformation of the carbon bridges makes a pseudo-rotation impossible, the asymmetric tilt (tilting of only one ferrocene unit) induces a twist. This tilt-induced twist has the same effect as in a *syn* conformer. Secondly, a symmetric tilt (tilting both the ferrocene units to the same degree, and in the same direction respectively, *e.g.* outwards) has the effect of making the carbon bridges come apart. This reduces the steric interaction between the *endo* methine protons in *e.g.* **3a** (*exo,exo,syn*) and is especially important in **3c** (*exo,endo,syn*) in order to reduce the steric repulsion between the *endo* methyl protons and the *endo* methine proton.

As can be seen from Table 5.3, the ferrocenophane part of the solid state structure of **2** in DMTHF does not differ much from the C_{2v} structure of the parent compound. That is, except for the bridge angle C2-C1-C22, which is 127° as compared with 122° in **1b**. This is interpreted as an effect of the change in hybridisation of C1.

5.2.5 Pseudo-rotation versus ring-inversion

Even if the conformational space of [1.1]ferrocenophane and cyclohexane are analogous, it does not mean that the inter conversion pathways have the same potential energy. Only the fact that the *syn* (boat) conformer of [1.1]ferrocenophane is the only one isolated in the solid state, tells us this. It seems that a twisted *syn*-structure has the lowest potential energy, but there cannot be large differences since it is possible to crystallise *anti*-isomers of DMFCP.

As of today, we have no evidence to indicate which mechanism for the internal inter conversions might be the preferred one. Is it pseudo-rotation or is it ring-inversion? The answer might be a bit of both, *i.e.* a pseudo-rotation with some ferrocene tilting.

Rudzinski and coworkers, have attempted to calculate the potential energy for the *syn-syn* inter conversion of **1**, with molecular mechanic methods.[98-100] The computed activation energy, 45 kJ mol^{-1},[99] is somewhat higher than our experimental value of 28 kJ mol^{-1}. The process for which this activation energy was calculated, seems to be a ring-inversion.

Our attempts to use *ab initio* calculations for problems relating to [1.1]ferrocenophane chemistry, have not been successful so far. The most promising attempt, has been the use of IGLO (Individual Gauge for Localised Orbitals) to calculate ^{13}C chemical shifts based on "X-ray structures".[101] These chemical shifts are then supposed to be compared with solid state NMR data. It is possible to handle [1.1]ferrocenophane in *e.g.* Gaussian 92. However, at this stage, the problem lies in insufficient convergence tools in the IGLO program.

Still, my hope is that computational chemistry, in some form, may be able to model the [1.1]ferrocenophane system well enough to give us the answers in the future. However, a number of problems are currently encountered, such as the lack of well-developed molecular mechanics parametrisation, the size (> 200 electrons), and the notorious difficulties in *ab initio* calculations on ferrocene itself.[102] One might, however, hope that the experimental data gathered so far in the [1.1]ferrocenophane system and the parallels that can be drawn with the cyclohexane system, will be an incentive to advance the computational methods sufficiently in order to handle this kind of system.

6. References

1. Dagani, R. *Chem.& Eng.News* **1982**, 23.
2. Mueller-Westerhoff, U. T.; Nazzal, A.; Prössdorf, W. *J. Am. Chem. Soc.* **1981**, *103*, 7678.
3. Ahlberg, P.; Davidsson, Ö.; Ewen, I. M.; Rönnqvist, M. *Bull. Soc. Chim. Fr.* **1988**, 177.
4. Ahlberg, P.; Davidsson, Ö. *J. Chem. Soc., Chem. Commun.* **1987**, 623.
5. Davidsson, Ö. Thesis, Göteborg University, 1990.
6. Johnson, C. K. ORTEP. Report ORNL-3794; Oak Ridge National Laboratory, Oak Ridge, TN, 1965.
7. Watts, W. E. *J. Organomet. Chem.* **1967**, *10*, 191.
8. McKechnie, J. S.; Berstedt, B.; Paul, I. C.; Watts, W. E. *J. Organomet. Chem.* **1967**, *8*, 29.
9. McKechnie, J. S.; Maier, C. A.; Bersted, B.; Paul, I. C. *J. Chem. Soc. Perkin Trans. 2***1973**, 138.
10. Barr, T. H.; Lentzner, H. L.; Watts, W. E. *Tetrahedron* **1969**, *25*, 6001.
11. Cassens, A.; Eilbracht, P.; Nazzal, A.; Prössdorf, W.; Mueller-Westerhoff, U. T. *J. Am. Chem. Soc.* **1981**, *103*, 6367.
12. Rheingold, A. L.; Mueller-Westerhoff, U. T.; Swiegers, G. F.; Haas, T. J. *Organometallics* **1992**, *11*, 3411.
13. Trifonov, D. N.; Trifonov, V. D. *Chemical Elements. How they were discovered;* 2nd ed.; MIR Publishers: Moscow, 1982.
14. Schlenk, W.; Holtz, J. *Chem. Ber.* **1917**, *50*, 262.
15. Ziegler, K.; Colonius, H. *Anal. Chem.* **1930**, *479*, 135.
16. Wittig, G.; Pockels, U.; Droge, H. *Chem. Ber.* **1938**, *71*, 1903.
17. Gilman, H.; Morton, J. W. *Org. React.* **1954**, *8*, 258.
18. Gilman, H.; Langham, W.; Jacoby, A. L. *J. Am. Chem. Soc.* **1939**, *61*, 106.
19. Lambert, C.; Schleyer, P. v. R. *Angew. Chem., Int. Ed. Engl.* **1994**, *33*, 1129.
20. Lambert, C.; Kaupp, M.; Schleyer, P. v. R. *Angew. Chem., Int. Ed. Engl.* **1993**, *12*, 853.
21. Allred, A. L.; Rochow, E. G. *J. Inorg. Nucl. Chem.* **1958**, *5*, 264.
22. Wakefield, B. J. *Organolithium Compounds*; Pergamon Press: Oxford, 1974.
23. Wakefield, B. J. *Organolithium Methods*; Academic Press: London, 1988.
24. Stowell, J. C. *Carbanions in Organic Synthesis*; Wiley: New York, 1979.
25. Williard, P. G. In *Comprehensive Organic Synthesis*; B. M. Trost and I. Fleming, Ed.; Pergamon Press: Oxford, 1991; Vol. 1.
26. Schlosser, M. In *Modern Synthetic Methods*; R. Sheffold, Ed.; Verlag Helvetica Chimica Acta VCH: Basel Weinheim, 1992; Vol. 6; pp 227.
27. Brandsma, L.; Verkruijsse, H. *Preparative Polar Organometallic Chemistry 1*; Springer: Berlin, 1987.
28. Brandsma, L. *Preparative Polar Organometallic Chemistry 2*; Springer: Berlin, 1990.
29. Schlosser, M. In *Modern Synthetic Methods*; R. Sheffold, Ed.; Verlag Helvetica Chimica Acta VCH: BaselWeinheim, 1992; Vol. 6; Chapter II.14.
30. Schlosser, M. *Struktur und Reaktivität polare Organometalle*; Springer: Berlin, 1973, Chapter 3,4.
31. Shannon, R. D. *Acta Crystallogr., Sect. A: Found Crystallogr.* **1976**, *32*, 751.
32. Grunwald, E. *Anal. Chem.* **1954**, *26*, 1696.
33. Winstein, S.; Clippinger, E.; Fainberg, A. H.; Robinson, G. C. *J. Am. Chem. Soc.* **1954**, *76*, 2597.
34. Fuoss, R. M.; Sadek, H. *J. Am. Chem. Soc.* **1954**, *76*, 5897.
35. Fuoss, R. M.; Sadek, H. *J. Am. Chem. Soc.* **1954**, *76*, 5905.
36. Marcus, Y. *Ion Solvation*; Wiley: Chichester, 1985.
37. Boche, G. *Angew. Chem., Int. Ed. Engl.* **1992**, *31*, 731.

38. Cram, D. J.; Mateos, J. L.; Hauck, F.; Langemann, A.; Kopecky, K. R.; Nielsen, W. D.; Allinger, J.; *J. Am. Chem. Soc.* **1959**, *81*, 5774.
39. Hogen-Esch, T. E.; Smid, J. *J. Am. Chem. Soc.* **1965**, *87*, 669.
40. Hogen-Esch, T. E.; Smid, J. *J. Am. Chem. Soc.* **1966**, *88*, 307.
41. Hogen-Esch, T. E.; Smid, J. *J. Am. Chem. Soc.* **1966**, *88*, 318.
42. Sethson, I. Thesis, Umeå University, 1991 (and references therein).
43. Smid, J. *Angew. Chem., Int. Ed. Engl.* **1972**, *11*, 112.
44. Weiss, E. *Angew. Chem., Int. Ed. Engl.* **1993**, *32*, 1501.
45. Gschwend, H. W.; Rodriguez, H. R. *Org. React.* **1979**, *26*, 1-17.
46. Mallan, J. M.; Bebb, R. L. *Chem.Rev.* **1969**, *69*, 693.
47. Maercker, A. *Angew. Chem., Int. Ed. Engl.* **1987**, *26* 972.
48. Lipshutz, B. H.; Kozlowski, J. A.; Breneman, C. M. *J. Am. Chem. Soc.* **1985**, *107*,
49. Lambert, C.; Schleyer, P. v. R. In *Metoden Der Organischen Chemie (Houben-Weyl)*; M. Hanack, Ed.; Georg Thieme Verlag: Stuttgart, 1993; Vol. E 19d.
50. Maskill, H. *The physical basis of organic chemistry*; Oxford University Press: Oxford, 1989.
51. March, J. *Advanced Organic Chemistry: reactions, mechanisms, and structure;* 4th ed.; Wiley-Interscience publication: New York, 1992.
52. Miller, S. A.; Tebboth, J. A.; Tremaine, J. F. *J. Chem. Soc.* **1952**, 632.
53. Kealy, T. J.; Pauson, P. L. *Nature* **1951**, *168*, 1039.
54. Wilkinson, G.; Rosenblum, M.; Whitting, M. C.; Woodward, R. B. *J. Am. Chem. Soc.* **1952**, *74*, 2125.
55. Woodward, R. B.; Rosenblum, M.; Whitting, M. C. *J. Am. Chem. Soc.* **1952**, *74*, 3458
56. Smith, B. H. *Bridged Aromatic Compounds*; Academic Press: New York, 1964.
57. Watts, W. E. *J. Am. Chem. Soc.* **1966**, *88*, 855.
58. Bitterwolf, T. E.; Ling, A. C. *J. Organomet. Chem.* **1973**, *57*, C15.
59. Morrison, W. H.; Hendrikson, D. N. *Inorg. Chem.* **1975**, *14*, 2331.
60. Mueller-Westerhoff, U. T.; Eilbracht, P. *J. Am. Chem. Soc.* **1972**, *94*, 9272.
61. Mueller-Westerhoff, U. T. *Angew. Chem. Int. Ed. Engl.* **1986**, *25*, 702.
62. Kansal, V. K.; Watts, W. E.; Mueller-Westerhoff, U. T.; Nazzal, A. *J. Organomet. Chem.* **1983**, *243*, 443.
63. Sandström, J. *Dynamic NMR Spectroscopy*; Academic Press: London, 1982.
64. *Design and production by J-M Löwendahl and H Svensson.*
65. *The DNMR5 program was obtained through the Quantum Chemistry Program Exchange (QCPE), by T. Olsson, Department of Organic Chemistry at Chalmers University of Technology. T. O. compiled it to run on a VMS-platform and a HP-platform and added an input interface.*
66. Kaplan, J. I.; Fraenkel, G. *NMR of Chemically Exchanging Systems*; Academic Press: New York, 1980.
67. *The 1D NMR simulation program was part of the Varian VNMR-S program package and was run on a SUN-platform.*
68. *Solid state NMR spectroscopic studies were performed in cooperation with S. Schantz, Department of Polymertechnology, Chalmers University of Technology.*
69. Gilmore, C. J. *J. Appl. Crystallogr.* **1984**, *17*, 42.
70. TEXSAN-TEXRAY Structure Analysis Package. Molecular Structure Corp., The Woodlands, TX, 1989.
71. *X-diffraction studies were performed in cooperation with M. Håkansson, Department of Inorganic Chemistry, Chalmers University of Technology.*
72. Rzepa, H. S.; Whitaker, B. J.; Winter, M. J. *J. Chem. Soc., Chem. Commun.* **1994**, 1907
73. Casher, O.; Chandramohan, G. K.; Hargreaves, M. J.; Leach, C.; Murray-Rust, P.; Rzepa, H. S.; Sayle, R.; Whitaker, B. J. *J. Chem. Soc. Perkin Trans. 2* **1995**, 7.
74. Chem3D *Cambridge Scientific Computing, Inc.*
75. Ball&Stick *Cherwell Scientific Publishing Limited.*

76. MacMimic *InStar Software AB*.
77. RasMac *Roger Sayle, BioMolecular Structures Group Glaxo Research & Development, Greenford, Middlesex, UK. (public Domain) ftp.dcs.ed.ac.uk*.
78. *Design and production by J-M Löwendahl and H Svensson.*
79. Le Vanda, C.; Bechgaard, K.; Cowen, D. E.; Mueller-Westerhoff, U. T.; Eilbracht, P.; Candela, G. A.; Collins, R. L. *J. Am. Chem. Soc.* **1976**, *98*, 3181.
80. Hafner, K.; Vöpel, K. H.; Ploss, G.; König, C. *Org. Syn., Coll. Vol. V,* 431.
81. Rausch, M. D.; Ciapenelli, D. J. **1976**, *10*, 127.
82. Walczack, M.; Walczack, K.; Mink, R.; Rausch, M. D.; Stucky, G. *J. Am. Chem. Soc.* **1978**, *100*, 6382.
83. Reiffers, S.; Vaalburg, W.; Wiegman, T.; Molen, H. D. B.-V. d.; Paans, A. M. J.; Woldring, M. G.; Wynberg, H. *J. Labelled Comp. Radiopharm.* **1979**, *26*, 56.
84. Negishi, E.; Swanson, D. R.; Rousset, C. J. *J. Org. Chem.* **1990**, *55*, 5406.
85. Baily, W. F.; Punzalan, E. R. *J. Org. Chem* **1990**, *55*, 5404.
86. Håkansson, M. *Inorg. Synth.*, Submitted for publication.
87. Bauer, W.; Winchester, W. R.; Schleyer, P. v. R. *Organometallics* **1987**, *6*, 2371.
88. Bauer, W.; Schleyer, P. v. R. *Adv. Carbanion Chem.* **1992**, *1*, 89.
89. *The simulations have been done with both DNMR5 and the program developed by G. Fraenkel and coworkers. We thank G. Fraenkel and A. Chow for their help with simulations*.
90. Anet, F. A. L.; Bourn, A. J. R. *J. Am. Chem. Soc.* **1967**, *89*, 760.
91. Burkert, U.; Allinger, N. L. *Molecular Mechanics*; American Chemical Society: Washington D.C., 1982.
92. Eliel, E. L.; Wilen, S. H.; Mander, L. N. *Stereochemistry of Organic Compounds*; John Wiley & Sons, Inc.: New York, 1993,.
93. Cremer, D.; Szabo, K. J. In *Conformational Behaviour of Six-Membered Rings: Analysis, Dynamics and Stereoelectronic Effects*; E. Juaristi, Ed.; VCH Publishers: in press.
94. Sachse, H. *Ber. Deut. Chem. Gesell.* **1890**, *23*, 1363.
95. Sachse, H. *Z. physik. Chem.* **1892**, *10*, 203.
96. Consulting of Mathematics and Statistics at the Centre of Applied Mathematics and Statistics, *Göteborg University. and Chalmers University of Technology.* http://www.math.chalmers.se:80/~konsult/
97. Watts, W. E. *Organomet. Chem. Rev.* **1967**, *2*, 231.
98. Rudzi´nski, J. M.; Ösawa, E.; Hisatome, M.; Watanabe, J.; Yamakawa, K. *J. Phys. Org. Chem.* **1989**, *2*, 602.
99. Rudzi´nski, J. M.; Ösawa, E. *J. Phys. Org. Chem.* **1992**, *6*, 107.
100. Rudzi´nski, J. M.; Ösawa, E. *J. Phys. Org. Chem.* **1992**, *5*, 382.
101. *The ab initio calculations have been done in cooperation with the grpoup of Prof. D. Cremers Department of Theoretical Chemistry at Göteborg University. Special thanks to L. Olsson and H. Ottosson.*
102. Park, C.; Almlöf, J. *J. Chem.Phys.* **1991**, *95*, 1829.

7. Articles

I. Monomeric 'Benzyl Lithium' in 2,5-Dimethyltetrahydrofuran. NMR Spectroscopic Studies of ^{6}Li and $^{13}C_2$ Labelled Ferrocenophanyl Lithium using ^{13}C-^{6}Li Coupling and ^{6}Li Decoupling

Öjvind Davidsson, Martin Löwendahl and Per Ahlberg.

J. Chem. Soc., Chem. Commun. **1992**, 1004-1005.

II. Crystal Structure of Ferrocenophanyllithium: Absence of an Intramolecular C-H...-C Hydrogen Bond

Per Ahlberg, Öjvind Davidsson, Göran Hilmersson, Martin Löwendahl and Mikael Håkansson.

J. Chem. Soc., Chem. Commun. **1994**, 1573-1574.

III. Catalysis of an Alkalimetallation Reaction - Mechanistic Studies of the Intramolecular Degenerate Rearrangement of [1.1]ferrocenophanyllithium.

Öjvind Davidsson, Martin Löwendahl, Göran Hilmersson and Per Ahlberg.

J. Am. Chem. Soc., submitted for publication.

IV. Pseudorotation in [1.1](1.1')Ferrocenophane, a Molecular Acrobat: a Study by Dynamic ^{1}H Nuclear Magnetic Resonance Spectroscopy

Martin Löwendahl Öjvind Davidsson and Per Ahlberg.

J. Chem. Research (S) **1993**, *1*, 40-41.

V. A *syn*-[1.1]Ferrocenophane with Approximate C_{2v} Symmetry

Mikael Håkansson, Martin Löwendahl, Öjvind Davidsson and Per Ahlberg.

Organometallics **1993**, *12*, 2841-2844.

VI. First Evidence for a Carbon-Bridged [1.1]Ferrocenophane in the *anti* Conformation. Molecular Structure of *exo,exo,anti*-1,12-Dimethyl[1.1]ferrocenophane

Martin Löwendahl, Öjvind Davidsson, Per Ahlberg, and Mikael Håkansson.

Organometallics **1993**, *12*, 2417-2419.

VII. 1,12-Dimethyl[1.1]ferrocenophane - an Organometallic Cyclohexane Analogue with Extraordinary Flexibility. Molecular Structure of a Third Isomer: *exo,endo,syn*-1,12-Dimethyl[1.1]ferrocenophane.

Jan-Martin Löwendahl and Mikael Håkansson.

Organometallics, submitted for publication.

GÖTEBORGS UNIVERSITET
GÖTEBORGS UNIVERSITETSBIBLIOTEK